An Analytical Approach to Computer Aided Diagnosis and Tuning of Lossy Microwave Coupled Resonator Filters

MENG, Meng

A Thesis Submitted in Partial Fulfillment

of the Requirements for the Degree of

Master of Philosophy

in

Electronic Engineering

The Chinese University of Hong Kong
July, 2009

I certify that I have read this dissertation and that in my opinion it is fully adequate, in scope and quality, as dissertation for the degree of Master of Philosophy.

(typed name) Principal Advisor

I certify that I have read this dissertation and that in my opinion it is fully adequate, in scope and quality, as dissertation for the degree of Master of Philosophy.

(typed name)

I certify that I have read this dissertation and that in my opinion it is fully adequate, in scope and quality, as dissertation for the degree of Master of Philosophy.

(typed name)

Approved for the University Committee on Graduate Studies

ABSTRACT

Microwave filter is a compulsory component in any communication system. In many complex frequency division architecture, filters are integrated with manifold to form a multiplexer (including a diplexer). In a multiplexer, the response of a channel filter is no longer an idea equal-ripple type, which drastically increases the difficulty of filter tuning. This thesis presents a novel analytical approach for extracting the coupling matrix of a narrow band general Chebyshev band pass filter with low to medium losses. The approach is very useful for computer aided tuning of a microwave band pass filter. The phase loading concept is materialized for the first time in the subject of computer aided tuning. The analytical approach consists of three aspects: (1) a theoretic formula that leads to a practical scheme for determining the phase loading; (2) a theoretic formula for de-embedding the section of unwanted transmission lines at the two ports of a filter; and (3) a theory for determining the unloaded Q of a filter; all from a given set of measured filter response. To make the approach easy to use, some practical techniques for reconstructing Y-parameters from a set of filter response by rational functions are also provided in the paper. The proposed diagnosis approach is highly applicable to a general coupled resonator filter with losses and therefore can be effectively used in computer aided tuning of a high order practical filter with cross couplings.

论文摘要

滤波器是通讯系统中的一个必要组件。在许多复杂的分频系统中，多功器是由通道滤波器集合而成的。在多功器的综合里，由于通道滤波器的响应不再是传统的 Chebyshev 曲线，滤波器的调试变得非常复杂。本论文提出了一种新型的解析的方法，用于提取窄带有损广义 Chebyshev 滤波器的耦合矩阵。这种方法可以有效地应用在滤波器的计算机辅助调试中。本论文在耦合矩阵的解析提取方面在三个方面做出了新的贡献：（1）提出了‘相位负载（phase loading）’的概念及解析提取的方法；（2）解析传输线 de-embedding 的方法；以及，（3）解析提取损耗滤波器无载 Q 值的方法。文中通过对具体实际例子的讨论证明了这种方法对于有损的，高阶的，有交叉耦合的滤波器的耦合矩阵提取的有效性。

ACKNOWLEDGMENTS

The author would like to express her sincere gratitude to her supervisor Professor Ke-Li Wu for his guidance on the research and study which makes this thesis possible, for his ways of logical thinking which has been a great value and for his motivation throughout the work. The author would like to thank her colleagues: Mr Huang Xiaobo, Mr Hu Hai as well as her other labmates in Microwave laboratory for their advice, support and friendship. The author owes her special thanks to Mr. Richard Cameron who inspires her with not only the knowledge in the field but also the attitude toward work.

DEDICATION

The author wishes to dedicate this dissertation to her parents.

TABLE OF CONTENTS

LIST OF TABLES

LIST OF FIGURES

Chapter 1

INTRODUCTION

The microwave spectrum is a finite resource which must be divided, cared for, and treated with respect.

— Dr. Leo Young

1.1 OVERVIEW OF MICROWAVE FILTERS

Microwave filter is a frequency selective device which passes signals of certain frequencies and blocks or attenuates signals of other frequencies. It is a compulsory component in any communication system. In many complex frequency division architectures, filters are integrated with manifold to form a multiplexer. Fig.1.1 shows a typical multiplexer used for satellite communication system.

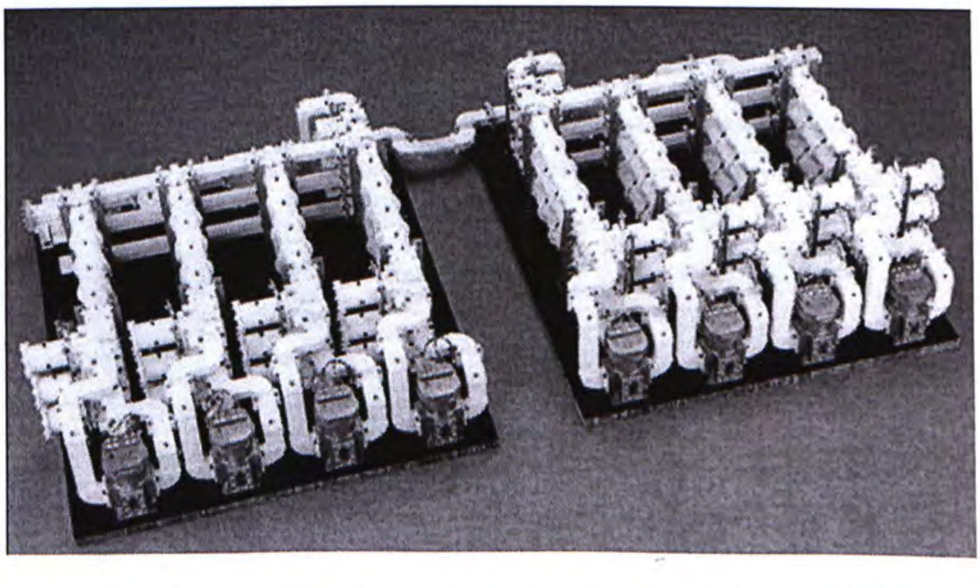

Fig. 1.1: Ku band input multiplexer sybsystem (Courtesy of COM DEV)

Modern filter theory has been developed since the early work in 1930s by Cauer, Darlington, and others. The problem of filter synthesis mainly involves two parts, (1) the approximation of the filter specifications by a transfer function; and (2) the design of a network which can realize the transfer function as illustrated in Fig.1.2. While the first part is solved by optimization, and the second one is solved with the knowledge of network synthesis.

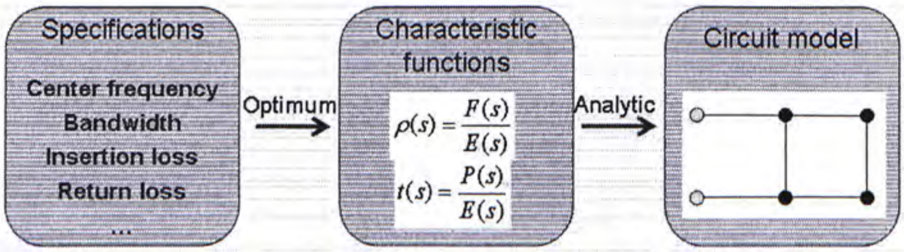

Fig. 1.2: Procedures of the design of prototype network

The prototype network can then be transformed into a variety of microwave networks including TEM transmission lines, waveguides and dielectric resonators. Fig. 1.3 shows the typical design process of a resonator with input and output couplings using an electromagnetic (EM) simulator.

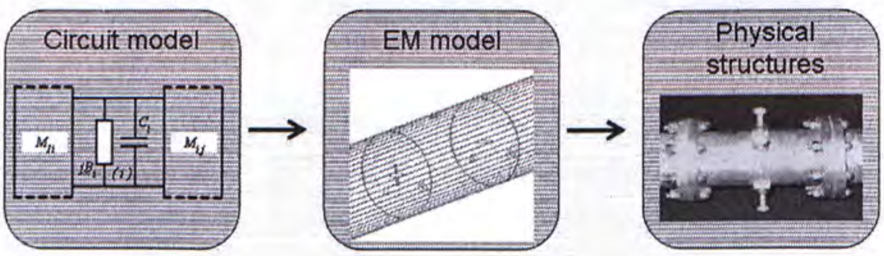

Fig. 1.3: The design process of resonators with couplings

1.2 TUNING OF MICROWAVE FILTERS

In order to accurately achieve a desired electric performance of a microwave coupled resonator filter, an effective tuning is a critical and compulsory step in both filter design and production. Nowadays, filter design utilizing EM simulators begins with the modeling and synthesizing the resonators and couplings separately. Connecting these parts together can only give an initial design. Tuning tools must be applied to get the desired properties based on the initial design.

When a filter is fabricated according to the electromagnetically designed model, tuning is again a necessary procedure to compensate manufacturing tolerances and uncertainties of materials such as the dielectric constant of a dielectric resonator. This situation is particularly true for narrow band general Chebyshev filters in a multiplexer of a satellite microwave payload.

The traditional tuning skill of a human operator is mainly built-up based on the fuzzy logics that he or she has accumulated over years. Because it requires enough experience to acquire the logic knowledge, the tuning process for high order filters with multiple cross-couplings becomes very labor intensive and expensive. Nevertheless, one of the difficulties associated to the traditional tuning is that it is not a deterministic process. In other words, there is no guaranty that each step of a tuning is always in the right direction. Such predicament is particularly undesirable in tuning a channel filter for satellite applications as a repeated tuning may wear out the plated silver of tuning screws and degrade the unloaded Q of the filter.

Due to the difficulties involved in the manual tuning, computer-aided tuning (CAT) of a microwave coupled resonator filter would be a more effective alternative, and it has drawn a great deal of attentions in recent years. Computer-aided tuning can be categorized into curve fitting method and parameter extraction method.

The first method, as indicated by its name, tunes the resonator and couplings sequentially so that the critical curve would be the same as that of the prototype network. For examples, the group delay response as shown in Fig.1.4 of each sub-circuit is used for the tuning of each coupling element and resonator one by one [1] , and parameter extraction is applied at tuning of each "sub-filter" using non-linear optimization [2]. The sequential tuning in time domain as shown Fig.1.5 is also an effective approach to bring a strongly detuned in-line coupled resonator filter into resonance [3]. The major difficulties that come with these sequential tuning schemes are (1) it is difficult to deal with cross coupling in general; (2) it is not always convenient to segregate each resonator or coupling element in a filter structure such as dielectric resonator filters; and (3) there is an accumulated error.

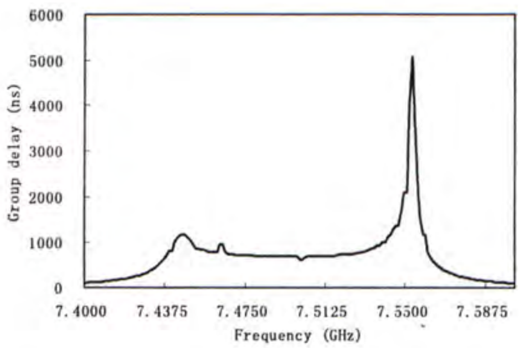

Fig. 1.4: Typical group delay response of a coupled resonator filter.

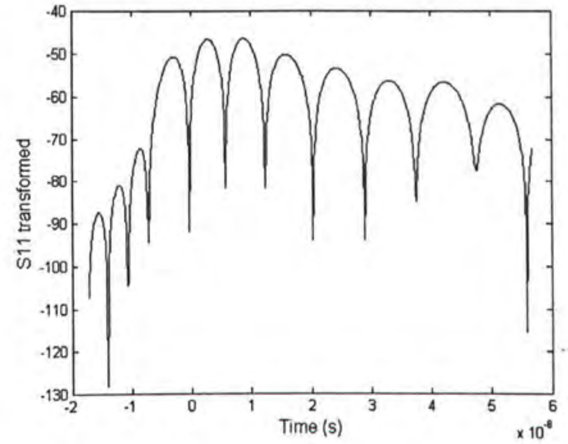

Fig. 1.5: Typical time domain response of a coupled resonator filter.

The basic idea of parameter extraction is to extract critical parameters such as the resonant frequencies and coupling values from measured data and tune the filter according to the different of the extracted ones and the designed ones. Many techniques have been proposed to determine parameters from measurement, and most of them utilize an optimization routine. Nonlinear optimization is a popular method used in industry for extracting the entire coupling matrix in one run from the measured filter responses [5]. The extracted coupling matrix (CM) can be used to identify the coupling elements that have large discrepancies as compared to the desired coupling matrix [6-8]. Due to the complexity of this kind of problem, the optimization procedures are either time consuming (for global optimization) or are very sensitive to the initial values and the number of variables (for gradient based local optimization), and is easily tripped into a local optimum.

The coupling matrix (CM) of a coupled resonator bandpass filter is a reference in describing the relationship between a physical realization and required filter response as each of the coupling elements in a CM uniquely corresponds to a physical tuning element; in addition, exact mathematic relation between transfer function and coupling matrix can be found [4]. The difference between the extracted one and the golden template will tell which tuning elements should be changed. The efficiency of this method depends on the accuracy of the modeling of a physical structure by a coupling matrix.

In theory, a coupling matrix is determined by the system poles and zeros (or the residues of the poles) for a given filter topology. It is assumed that the multiple solution problem is not a concern in the discussion as a computer aided tuning process always leads the CM to the desired physical solution in practice. For some simple filter configurations, in which each coupling element and resonator can be easily isolated, some analytic formulas have been reported for determining the CM, For examples, works in [9, 10] provided a method that associates the poles and zeros of reflection coefficients with the CM for cascaded and symmetrically coupled filters. A special attention must be drawn here to the fact that the phase derivative with respect to frequency is used in [9, 10] for accurately determining the system poles and zeros and in [1] for correlating the coupling values in the circuit model with those in the physical model through group delay information. Poles and zeros of Y parameters are investigated in [11] because they have direct relations to the canonical coupling matrix.

1.3 RATIONALIZATION OF MEASURED DATA

In a filter diagnosis using coupling matrix extraction, one must convert filter responses of a physical model (a measured or EM simulated response) into the domain of a filter circuit model. Nevertheless, one needs to realize that measured response is not necessarily the same as a filter's circuit model. While resonator frequencies and the values of all the couplings in a circuit model and a physical model match to each other perfectly, the phases of the scattering parameters between the input and the output in the two models are not. In a circuit model, I/O couplings are two ideal frequency invariant inverters as shown in Fig.1.6; while in a physical model, the two couplings are realized by more complicated structures situated by stored electromagnetic energy of higher order modes, which can not be fitting into a circuit model of lumped elements.

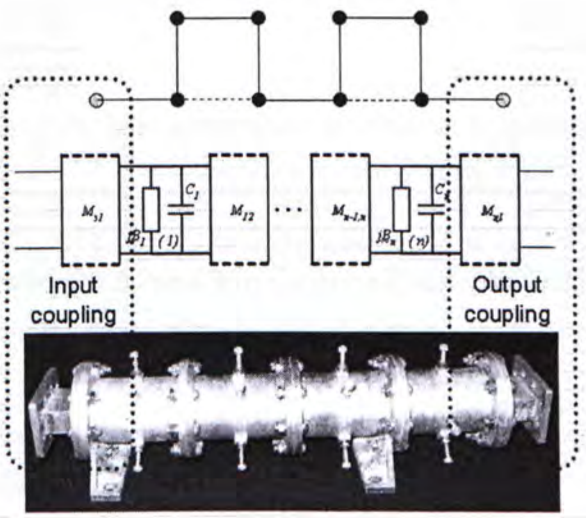

Fig. 1.6: The input and output couplings in circuit model and physical model.

As a result, in real time measurement, the tuning procedure begins with a conversion of a physical model of a measured data into the rational model that can be represented by a coupling matrix. The conversion comprises the removal of three non-ideal effects in the raw measured data from a physical filter model: (1) a section of embedded transmission line at each port of a filter; (2) a constant phase loading that is caused by stored energy in the vicinity of discontinuities; and (3) the loss effect associated to the unloaded Q of each resonator.

In [9], a length of transmission line at input port is determined by comparing measured response of the first resonator with the ideal condition. This method is difficult when we deal with dielectric filters or waveguide filter because it is not easy to detach the first cavity. In [12], the reference plane is adjusted by fitting S parameters outside the passband. We present a method for de-embedding by modeling the phases of resonator filter itself and the influences of transmission line.

Due to the stored energy of higher order modes at the input and output ports of a filter, it is the first time to find that there is a constant phase difference between the measured filter responses and those of the rational polynomial representation. Fail to remove the phase loading will lead to false determination of poles and zeros of Y parameters. This important concept has been ignored in all the existing CAT techniques. The original concept of a constant phase loading was first proposed by the Meng and Wu in [11], also phase loading is chosen as constant values which make the product sum of eigenvalue-residue reach to its minimum. This method for determining the values of phase loading may take lots of time because for every testing value a complete extraction is needed. However, the work in [11] only justified the existence of a constant phase loading mathematically without showing how to determine it. Secondly, the work only presented an analytical diagnosis scheme for lossless case. These two major shortcomings in [11] restrict the analytical CAT approach from practical uses.

1.4 CONTRIBUTIONS OF THIS THESIS

In this thesis, a novel analytical diagnosis and computer aided tuning approach for a general Chebyshev coupled resonator filter with low to medium loss is presented for the first time in the subject of CAT.

- It is the first time to emphasis the crucial impact of data rationalization on filter diagnosis based on coupling matrix. By analyzing basic properties of circuit model and physical filter, an effective step by step procedure is presented to derive rational responses from measurement that are consistent with those of a circuit model.

- In the prior parameter extraction methods, much of the attention is paid to the magnitude of S parameters while the phases are neglected. The rationalization of measured data discussed in Chapter 3 concerns much with the phases which are indispensable in order to appreciate adequately full descriptions of filters' characteristics.

- The concept of a constant 'phase loading' is materialized for the first time. A practical and simple-to-operate analytical scheme for removing the phase loading is proposed, which is crucial for revealing all the systematic poles and extracting a coupling matrix with physical meaning.

- An approximate formula is derived for deterministically de-embedding the section of unwanted transmission line or waveguide from measured S-parameters.

- With the rationalized S parameters, the original problem of parameters extraction which can only be solved by optimization is equivalently converted to a linear system problem which can be solved by analytical method even when loss is considered.

  - A novel theory of extracting filters' loss factors and corresponding coupling elements from the measured data is developed in this thesis for the first time.

  - In order to make the presented coupling matrix extraction method robust, issues dealing with the degenerate poles and measurement noise are also addressed.

- A large number of practical measured and simulated examples are given to illustrate the implementation of the approach and to demonstrate the validation of the analytical approach in practical uses.

Using the presented approach, there is no need to run any optimization routines and no requirement for initial values. The diagnosis and tuning of a practical Chebyshev coupled resonator filter become deterministic and easy-to-operate. With connection to network analyzer through a cable and the GPIB interface, the tuning and diagnosis could run in real time. It is expected that the proposed analytical approach can significantly accelerate the tuning of the high-order Chebyshev coupled resonator filters particularly in a deterministic way, and can become a very useful tool in the filter and space microwave payload industries. Under some extreme cases where analytic extraction can not meet the needs, it can provide at least a very good initial value for further non-linear optimization.

1.5 ORGANIZATION OF THIS THESIS

In chapter 2, procedures of coupling matrix extraction are given. The discussion begins with the easiest case in which filters' responses are lossless. Then the method for determining loss is discussed. Finally, solutions to degenerated poles are included. Chapter 3 provides processes for data rationalization. Influences of transmission line and phase loading during measurement are expressed by approximated functions. By analyzing basic properties of a circuit model, effects of transmission line and phase loading can be eliminated leaving rational data suitable for extraction. Chapter 4 presents four examples of coupling matrix extraction. Practical problems are discussed. Chapter 5 gives the strategies for the tuning of filters in different conditions including the ones just assembled showing no filter characteristics and the ones almost tuned. Three examples are given to illustrate the effectiveness and validation of the proposed approach. Appendix A presents the outline of time-domain method and Appendix B is the user's manual for the software the author developed which has been used by satellite microwave payload industry for the tuning of channel practical filters.

Chapter 2

COUPLING MATRIX EXTRACTION METHODS

The design of filters is unusual in that it uses network synthesis, with which it is possible to apply systematic procedures to work forward from a specification to a final theoretical design.

— Dr. Ian Hunter

This chapter provides a comprehensive discussion on the coupling matrix extraction of lossless and lossy Chebyshev narrow band filters. The discussion starts with an overview of coupling matrix in modern filter synthesis. Then methods for coupling matrix extraction is presented with three different cases: (1) the lossless case using the denominator and numerator of the admittance parameters; (2) the complex pole method to deal with loss and (3) the rational polynomial fitting method to deal with the case of degenerated poles.

2.1 BASICS FOR COUPLING MATRIX SYNTHESIS

The first part of this chapter is devoted for an overview of the synthesis of coupling matrix. It is well established that S parameters of doubly terminated lossless lowpass prototype filter networks can be expressed by characteristic polynomials as [13]

$$\begin{aligned} S_{11}(s) &= \frac{F(s)}{\varepsilon_R E(s)} \\ S_{21}(s) &= \frac{P(s)}{\varepsilon\ E(s)} \end{aligned} \tag{2.1}$$

where $F(s)$, $E(s)$ and $P(s)$ are finite degree polynomials with complex coefficients and their degrees corresponding to the order and number of transmission zeros of a filter.

With S parameters response measured from a network analyzer or EM simulation tools, the short circuit admittance parameters can be obtained [14] easily by (2.2). Throughout this thesis, while the data rationalization is an operation performed on S parameters, the coupling matrix extraction is based on the admittance parameters.

$$
\begin{aligned}
y_{11} &= \frac{(1-s_{11})(1+s_{22})+s_{12}s_{21}}{(1+s_{11})(1+s_{22})-s_{12}s_{21}} \\
y_{12} &= \frac{2s_{12}}{(1+s_{11})(1+s_{22})-s_{12}s_{21}} \\
y_{21} &= \frac{2s_{21}}{(1+s_{11})(1+s_{22})-s_{12}s_{21}} \\
y_{22} &= \frac{(1+s_{11})(1-s_{22})+s_{12}s_{21}}{(1+s_{11})(1+s_{22})-s_{12}s_{21}}
\end{aligned}
\tag{2.2}
$$

With measured S parameters, short circuit admittance parameters with respect to low pass frequency variable ω can be derived easily using band pass to low pass transformation as[13]:

$$
\omega = \frac{\omega_0}{\omega_2 - \omega_1}\left(\frac{\omega_b}{\omega_0} - \frac{\omega_0}{\omega_b}\right) \tag{2.3}
$$

where ω_0 is the center frequency of the pass band, ω_b is the bandpass frequency variable, ω_1 and ω_2 are lower and upper band edge frequencies.

Partial fraction expressions of the short circuit admittance matrix of an Nth degree filter contain N single-pole terms and can be written as [4]:

$$[Y_N]=\begin{bmatrix} y_{11}(s) & y_{12}(s) \\ y_{21}(s) & y_{22}(s) \end{bmatrix}=\sum_{k=1}^{N}\frac{1}{s-j\lambda_k}\begin{bmatrix} r_{11k} & r_{12k} \\ r_{21k} & r_{22k} \end{bmatrix} \tag{2.4}$$

where $j\lambda_k$ is the pole of the kth term, r_{11k} r_{21k} and r_{22k} are the residues of Y_{11}, Y_{21} and Y_{22}. The necessary and sufficient conditions that the admittance parameters can be realized by a lossless circuit model and can be represented by a coupling matrix are [15]:

(1) the poles $j\lambda_k$ are purely imaginary satisfying:

$$\sum_{k=1}^{n} j\lambda_k = 0 \tag{2.5}$$

(2) the residues of the Y_{11}, Y_{22} are real and positive while the residues of Y_{21} are real, and they must satisfy:

$$\begin{aligned} &\sum_{k=1}^{n}\lambda_k r_{11k}=\sum_{k=1}^{n}\lambda_k r_{22k}=0 \\ &\sum_{k=1}^{n} r_{21k}=0 \end{aligned} \tag{2.6}$$

In the sense of partial fraction expansion, one filter can be fully determined by its poles and residues of admittance parameters. The N+2 fully-canonical coupling matrix can also be derived from the residues and poles. Then similarity transformations can be applied to the canonical matrix so that desired configuration can be achieved.

$$CM=\begin{bmatrix} 0 & M_{s1} & M_{s2} & \dots & M_{sN} & 0 \\ M_{s1} & M_{11} & & & & M_{L1} \\ M_{s2} & & M_{22} & & & M_{L2} \\ \dots & & & \dots & & \dots \\ M_{sN} & & & & M_{NN} & M_{LN} \\ 0 & M_{L1} & M_{L2} & \dots & M_{LN} & 0 \end{bmatrix} \quad \begin{aligned} M_{Lk} &= \sqrt{r_{22k}} \\ M_{Sk} &= r_{21k}\Big/\sqrt{r_{22k}} \\ M_{kk} &= -\lambda_k \end{aligned} \tag{2.7}$$

In the following sections, methods for extracting CM of three different cases are developed. The first case illustrates basic procedures of CM extraction using lossless circuit model or EM model responses; the second case deals with lossy response which is more practical; and the third case discusses the solution to a degenerated pole response using higher order filter. Those methods share the same basic procedures. Different algorithms are applied for determining the values of its eigenvalues and residues.

2.2 LOSSLESS COUPLING MATRIX EXTRACTION

In general, the recovery of a CM from measured data using Y parameters requires three steps: (1) find the poles of Y parameters and construct the denominator; (2) determine the residues of admittance parameters according to the recovered numerator polynomials; (3) transform the canonical CM built up by poles and residues into the desired configuration.

In the discussion of lossless coupling matrix extraction, a circuit model of a 4^{th} degree filter is used as an example to illustrate the procedures. For the response of a circuit model, by nature rational, the locations of the peaks in the admittance parameters as shown in Fig.2.0 indicate the poles of the rational polynomials and are actually the eigenvalues of the coupling matrix.

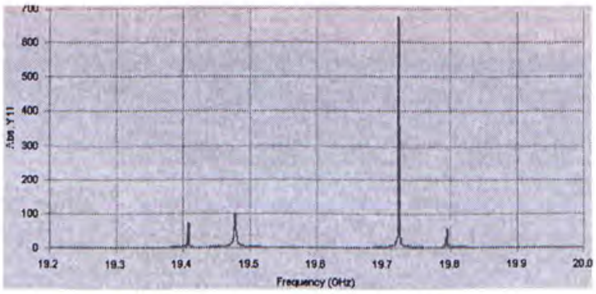

Fig. 2.0: The Absolute value of Y11 of a 4^{th} degree filter using the circuit model.

With the positions of poles, the explicit polynomial expression for the denominator can be found easily as

$$Y_{d11} = \prod_{j=1}^{n} (\omega - \lambda(i)) \tag{2.8}$$

The numerical values of the numerator of Y_{11} at every frequency except at poles can be determined by multiplying the numerical values of Y_{11} by the product of the denominator of each partial fraction such that

$$Y_{n11} = Y_{11} \prod_{i=1}^{n} (\omega - \lambda(i)) = \sum_{i=1}^{n} [r_{11}(i) \prod_{\substack{j=1 \\ j \neq i}}^{n} (\omega - \lambda(i)] \tag{2.9}$$

The numerator polynomial, which is a slow-variation function, can be found by least square fitting. The advantage of this treatment is

(1) Comparing to the method of fitting a function with multiple poles, the proposed approach is much easier because only a smooth function needs to be approximated by fitting.

(2) The degree of polynomial fitted is not limited here. This means that the accuracy of curve fitting can be increased because one can choose higher order polynomials.

Having determined the numerator and denominator of Y_{11}, when the frequency is equal to an eigenvalue, only one term is left and the corresponding residue can then be easily found, that is

$$\begin{aligned} &when \quad \omega = \lambda(i) \\ &Y_{n11}(\lambda(i)) = r_{11}(i) \prod_{\substack{j=1,n \\ j \neq i}} (\omega - \lambda(j)) \end{aligned} \tag{2.10}$$

Since the curve of the numerator polynomial is a smooth function the polynomial expression of the numerator can be found accurately by a simple least square fitting. Spikes may show in recovered data simply because the admittance parameter at pole is multiplied by zero. In the curve fitting process, as long as one chooses sample points by avoiding those positions, the matching is acceptable. Fig. 2.1 shows the fitting of the numerator of Y_{11} using polynomials.

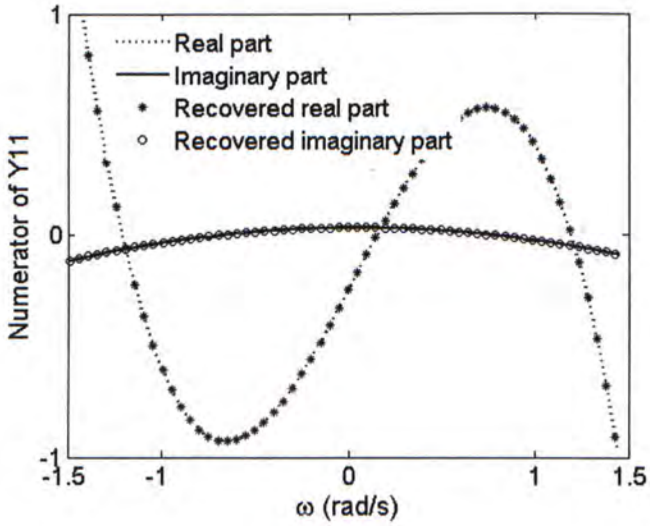

Fig. 2.1: The fitting of the numerator of Y_{11} using a 4th degree circuit filter model.

Having determined the polynomial expressions of the numerator and the denominator of Y_{11}, when the frequency is chosen to be equal to the value of a pole, the corresponding residue can be easily found as

$$r_{11}(i) = Y_{n11}(\lambda(i)) / \prod_{j=1,n;j\neq i} (\omega - \lambda(j)) \tag{2.11}$$

Fig. 2.2 shows the S11 from extraction and simulation.

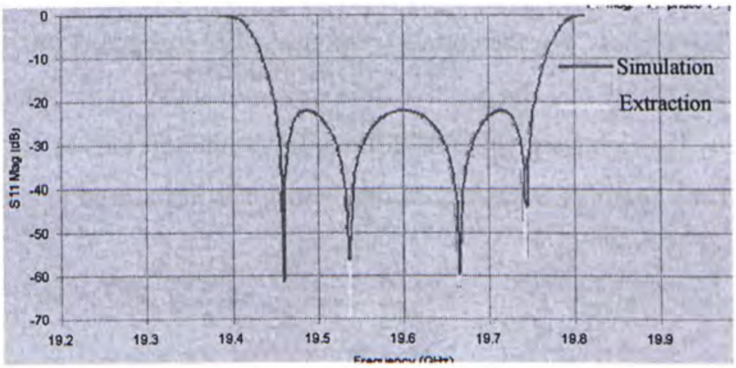

Fig. 2.2: The comparison between S11 of extraction and simulation.

This approach works accurately for lossless case. When there is loss, Y parameters will be complex numbers whose real parts represent the loss. If poles are treated as purely imaginary numbers as in the lossless case, the residues are responsible for the loss so they have to be complex. This violates the basic requirement for the residues of Y_{11} of realizable model that the residues of Y_{11} and Y_{22} should be purely real and positive. The details of how to deal with the lossy case will be discussed in next section. The residues of Y_{22} and Y_{21} can be found by the same token.

The successful application of this method in coupling matrix extraction is due to the fact that comparing to optimizing the whole coupling matrix, because the poles are given, it is much easier to determine only the residues. It is worth mentioning that the accurate results can only be achieved when the phase loading is removed properly.

2.3 LOSSY COUPLING MATRIX EXTRACTION

The values of Y_{11} at poles are infinite for lossless case. When losses are presented, admittance parameters will exhibit a real part. If poles are treated as purely imaginary numbers, the residues will be complex, which represent non-physical coupling elements of ordinary filters. For the coupled resonator filter concerned, the residues of Y_{11} and Y_{22} should be purely real and positive. It is well known that in the synthesis of a predistortion filter, by the rightward shifting of the poles on the left half of the complex plane, a real part of the complex frequency in denominator is introduced to compensate the effect of loss [14] as

$$Y_{11} = \sum_{i=1}^{n} \frac{r_{11}(i)}{(j\omega + \sigma(i)) - j\lambda(i)} \tag{2.12}$$

where σ is called the dissipation factor and is related to the fractional bandwidth and unloaded Q of the filter by

$$\sigma = \frac{f0}{BW} \cdot \frac{1}{Q_u} \tag{2.13}$$

Inspired by this treatment, the real part of the frequency variable is grouped into the pole values so that the effective loss of a filter can be taken into account by the real part of poles while the residues remaining to be positive real numbers.

$$Y_{11} = \sum_{i=1}^{n} \frac{r_{11}(i)}{j\omega - (j\lambda(i) - \sigma(i))} \tag{2.14}$$

2.3.1 Effects of dissipation factor

The admittance parameters can be separated into the real part and imaginary part. As shown in the partial expansion of the admittance parameters, the value of the admittance parameters near a pole is dominated by a single term, so the following approximations can be made:

$$\begin{aligned}\mathrm{Re}(Y_{11}) &= \sum_{i=1}^{n} \frac{r_{11}(i)\sigma(i)}{(\omega-\lambda(i))^2+\sigma(i)^2} \\ &\approx \frac{r_{11}(i)\sigma(i)}{(\omega-\lambda(i))^2+\sigma(i)^2} \le \left(\frac{r_{11}(i)}{\sigma(i)}\right)\end{aligned} \tag{2.15}$$

$$\begin{aligned}\mathrm{Im}(Y_{11}) &= \sum_{i=1}^{n} \frac{r_{11}(i)(\omega-\lambda(i))}{(\omega-\lambda(i))^2+\sigma(i)^2} = \sum_{i=1}^{n} \frac{r_{11}(i)}{(\omega-\lambda(i))+\dfrac{\sigma(i)^2}{(\omega-\lambda(i))}} \\ &\approx \frac{r_{11}(i)}{(\omega-\lambda(i))+\dfrac{\sigma(i)^2}{(\omega-\lambda(i))}} \le \left(\frac{r_{11}(i)}{2\sigma(i)}\right)\end{aligned} \tag{2.16}$$

The maximum values in the above relations are achieved when:

$$\mathrm{Re}(Y_{11}) \approx \left(\frac{r_{11}(i)}{\sigma(i)}\right)_{\omega=\lambda(i)} \tag{2.17}$$

$$\mathrm{Im}(Y_{11}) \approx \left(\frac{r_{11}(i)}{2\sigma(i)}\right)_{\omega=\lambda(i)\pm\sigma(i)} \tag{2.18}$$

Three important conclusions can be drawn from above two equations:

(1) a local maximum of magnitude of the real part of Y_{11} is achieved when the frequency equals to the imaginary part of a pole.

(2) when the frequency equals to the imaginary part of a pole the corresponding term in the imaginary part of Y_{11} goes to zero.

(3) the location of the local maximum of a term in the imaginary part at its corresponding pole is attained when the frequency is shifted away from the imaginary axis by amount of $\sigma(i)$, and the value of the maximum is half of that of the counterpart in the real part.

A two-step approach for accurately finding the complex poles of the admittance parameters is proposed. For a lossy bandpass filter, the scheme for determining the real positive residues discussed earlier is still applicable. The first step of the approach provides the initial values of the complex poles, and the second step is to fine tune the complex poles.

To continue with the earlier example, an equal unloaded Q is assigned to each resonator to introduce a loss into the system. With Qu=8000, Fig.2.3 shows the real and imaginary parts and their maximum values of the lossy model.

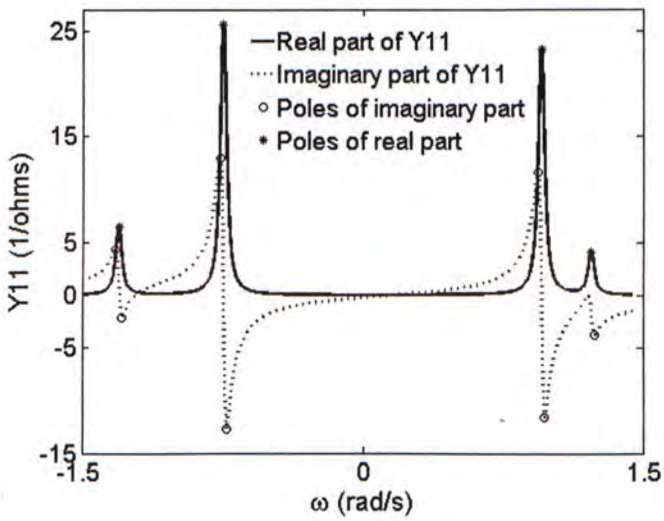

Fig. 2.3: Circuit model of lossy 4th degree filter with real and imaginary parts and their maximum values.

Now the question is how to find the proper complex poles to reconstruct the denominators of Y parameters so that the residue extraction method can be applied. The following three methods are provided for estimating the complex poles.

2.3.2 Determination of dissipation factor

Approximation method single pole

Since the loss factor σ(i) are usually small as compared to λ (i), when ω is near a pole, the i^{th} term in the partial fraction expression will dominate. Using eqs. (2.15) and (2.16), an approximated loss factor σ(i) can be found by the derivative of the ratio of the real and the imaginary parts of Y11 near the i^{th} pole as

$$\begin{aligned} &\omega \approx \lambda(i), \\ &\frac{\mathrm{Im}(Y_{11})}{\mathrm{Re}(Y_{11})} \approx \frac{r_{11}(i)(\omega-\lambda(i))}{(\omega-\lambda(i))^2+\sigma(i)^2} \Bigg/ \frac{r_{11}(i)\sigma(i)}{(\omega-\lambda(i))^2+\sigma(i)^2} \\ &= \frac{\omega-\lambda(i)}{\sigma(i)} \end{aligned} \tag{2.19}$$

So that the dissipation factor corresponding to the i^{th} pole can be approximated as:

$$\sigma(i) \approx \left(\frac{-d[\mathrm{Im}(Y_{11})/\mathrm{Re}(Y_{11})]}{d\omega} \right)^{-1} \tag{2.20}$$

Due to the limited accuracy of a numerical derivative near a pole, there are some slight discrepancies between the Y parameters of the physical model and that of the extracted rational model.

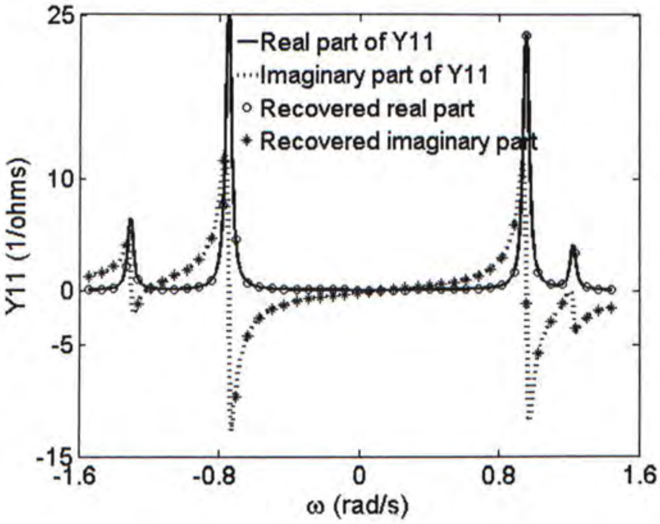

Fig. 2.4: Circuit model of a lossy 4 degree filter with Qu=8000 by fitting of Y_{11}, Y_{21}

Adjustment method by complex Y parameters

While the admittance parameters have infinite poles for lossless response, the values are finite when loss is introduced. Using the estimating method discussed earlier, one can derive values of finite Y parameters using complex poles. For the rational polynomial of Y parameters, the denominator Y_d is now given by

$$Y_d = \prod_{i=1}^{n} (j\omega - j\lambda(i) + \sigma(i)) \tag{2.21}$$

Then the polynomial of the numerator of Y parameters can be obtained by least square polynomial fitting as in the lossless case. Using the fitted values of the numerator, the values of the Y are derived at each frequency. As the magnitude of the Y parameter at a pole is mainly determined by the value of corresponding loss factor σ according to (2.21), if the imaginary part of the pole is accurately determined from the measured responses

(2.22), the loss factor σ(i) calculated can be fine tuned by matching the finite 'peak' values of the Y parameters from the measured data and the recovered ones(2.23).

$$Y_{11}(\lambda_i) \approx \frac{r_{11}(i)}{\sigma(i)} \tag{2.22}$$

$$\sigma'(i) = \frac{Y_{11\_mea}(\lambda_i)}{Y_{11}(\lambda_i)}\sigma(i) \tag{2.23}$$

The general procedure for determining CM using poles and residues of Y parameters is illustrated in the following flow chart.

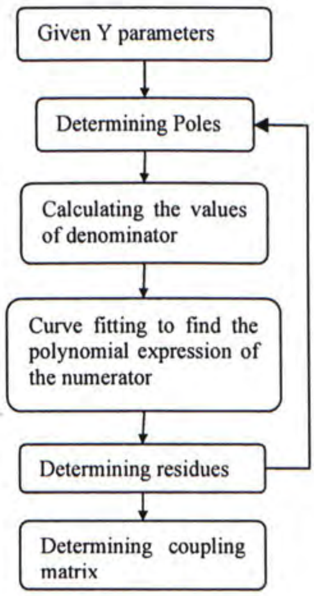

Although the residues found using the complex poles are still complex numbers, their imaginary parts are a few orders of magnitude smaller than that of the real parts. It can be observed in practice that when an appropriate loss factor is found, the absolute value of the imaginary parts of the residue reaches to its minimum as shown in Fig. 2.5.

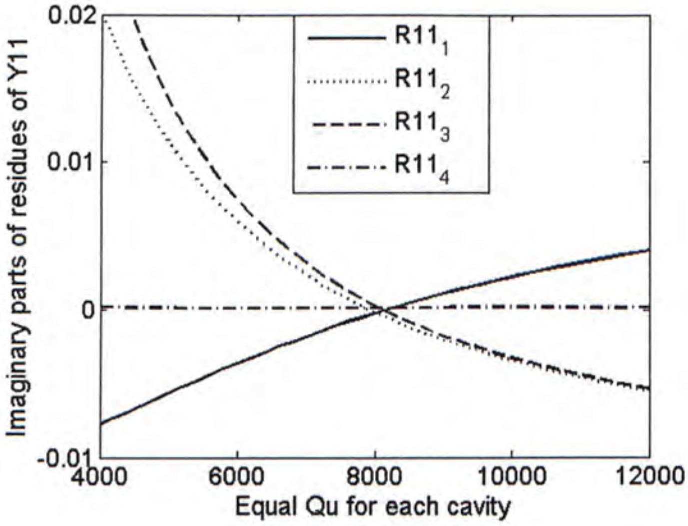

Fig. 2.5: Imaginary parts of residues with different Qu for a 4th degree circuit model with Qu=8000.

Table 1 shows the extracted poles and residues using three different methods for the 4th degree filter of circuit model.

Table 1: Poles and Residues Extracted (Designed Qu=8000)

Terms		1	2	3	4
Original	Pole	-1.3070	-0.7485	0.9523	1.2230
	Residues	0.1214	0.4821	0.4373	0.0765
Method I	Im. Poles	-1.3063i	-0.7480i	0.9544i	1.2228i
	Residues	0.121 +j4.1e-4	0.452 -j1.4e-2	0.426 -j1.2e-2	0.0562 -j1.5e-2
Method II	Re.Poles	0.0192	0.0192	0.0192	0.0192
	Residues	0.1228 -j4.8e-4	0.4835 -j1.3e-4	0.4377 -j6.0e-4	0.0742 -j1.0e-4
	Qu	7850	7850	7850	7850
Method III	Re.Poles	0.0190	0.0189	0.0189	0.0187
	Residues	0.1221 -j2.8e-4	0.4831 -j1.3e-4	0.4375 +j3.2e-4	0.0748 +j1.8e-4
	Qu	7919	7985	7997	8049

2.3.3 Coupling matrix synthesis method with loss

An (N+2) coupling matrix of a given filter responses can be constructed by the imaginary parts of poles and real residues. With complex poles, the CM can be also presented as a complex matrix. The imaginary part of the CM represents the coupling between coupled resonators for lossless case. The real part of the CM represents the loss of the filter and exhibits as a diagonal matrix. The two parts of the CM can be separated into two matrices as

$$\mathrm{Im}(CM)=\begin{bmatrix} 0 & \sqrt{R_{11}(1)} & \sqrt{R_{11}(2)} & \ldots & \sqrt{R_{11}(N)} & 0 \\ \sqrt{R_{11}(1)} & -\lambda(1) & & & & \dfrac{R_{21}(1)}{\sqrt{R_{11}(1)}} \\ \sqrt{R_{11}(2)} & & -\lambda(2) & & & \dfrac{R_{21}(1)}{\sqrt{R_{11}(1)}} \\ \ldots & & & \ldots & & \ldots \\ \sqrt{R_{11}(N)} & & & & -\lambda(N) & \dfrac{R_{21}(1)}{\sqrt{R_{11}(1)}} \\ 0 & \dfrac{R_{21}(1)}{\sqrt{R_{11}(1)}} & \dfrac{R_{21}(2)}{\sqrt{R_{11}(2)}} & \ldots & \dfrac{R_{21}(N)}{\sqrt{R_{11}(N)}} & 0 \end{bmatrix} \tag{1.24}$$

$$\mathrm{Re}(CM)=\begin{bmatrix} 0 & 0 & 0 & \ldots & 0 & 0 \\ 0 & \sigma(1) & & & & 0 \\ 0 & & \sigma(2) & & & 0 \\ \ldots & & & \ldots & & \ldots \\ 0 & & & & \sigma(N) & 0 \\ 0 & 0 & 0 & \ldots & 0 & 0 \end{bmatrix} \tag{1.25}$$

$$Q_u=\frac{f0}{BW}\cdot\frac{1}{\sigma} \tag{1.26}$$

For a given filter coupling topology, a sequence of same similarity transformations needs to be applied to the two matrices separately. As the result, the imaginary part of the coupling matrix reflects the actual couplings of a particular bandpass filter for a given response.

For an ideal case using circuit models, we can assign the same loss for each cavity. After extraction, the diagonal elements in the real matrix representing loss will have the same values. It is the product of an identity matrix and a constant, thus the similarity transformation based on matrix multiplication will not change this part of coupling matrix. Then we can calculate Qu for each cavity with the diagonal element.

The same example presented earlier is used again here. Table 2 lists the elements in CM from gold template and extraction. The S parameters extracted are compared to the ones from simulation in Fig. 2.6.

Table 2: Coupling elements extracted (Designed Qu=8000)

	M01	M12	M14	M22	M23	M24	M33	M34	M45
Ideal	1.0570	-0.8148	0.4699	0.2039	0.8416	0.2509	0.3409	0.7752	1.0570
Extracted	1.0571	-0.8143	0.4711	0.2074	0.8392	0.2564	0.3506	0.7733	1.0570

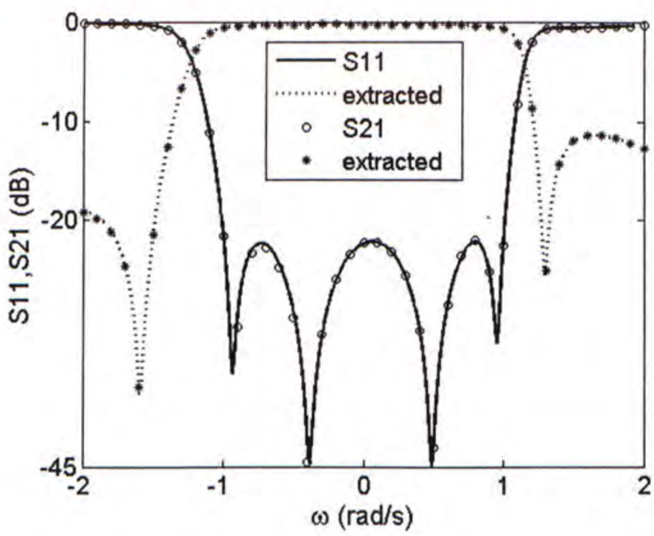

Fig. 2.6: S parameters and its recovery using a lossy 4th degree circuit model.

However, when the loss factors are not the same, the transformations will result in a full matrix. This means while the loss of N+2 original modal is constraint to cavities, the loss for real filter is distributed to cavities and every coupling even when the physical coupling is zero. From experience we know the losses for each resonator in a real filter do not varies too much. The more uniform the loss factors are, the more dominant the diagonal elements in the transformed matrix will be. In practice, because the loss among the resonators in a practical filter does not vary too much, the resultant off-diagonal elements in the transformed loss matrix can be ignored. Having had the transformed loss matrix, the unloaded Q for the i^{th} resonator can be found by where σ(i) is the i^{th} diagonal element of the transformed loss matrix.

An 8^{th} degree C-band filter is used to illustrate the concept mentioned earlier. To add loss into the EM model, the conductivity is set to be $4\times10^{7} S\cdot m^{-1}$. For a real filter, the loss of each resonator will not be the same, so the Q_us for the canonical N+2 coupling matrix and the ones after similarity transformations are different. The diagonal elements in Table 3 are 10 times larger than the other elements, and this ensures a reasonable accuracy of our operation. When the off-diagonal elements are neglected, loss of the entire structure is represented by the unloaded Q of each resonator.

Table 3: The Imaginary part of the extracted coupling matrix of the 8^{th} degree filter

0	0	0	0	0	0	0	0	0	0
0	-2.8e-2	6.6e-4	-2.2e-3	1.1e-3	-4.8e-4	-1.1e-3	1.3e-3	-8.0e-5	0
0	6.6e-4	-3.0e-2	1.7e-6	1.3e-3	3.9e-5	-3.8e-4	6.4e-4	-1.2e-3	0
0	-2.2e-3	1.7e-6	-2.7e-2	-1.9e-3	-7.6e-5	1.2e-3	2.7e-4	-9.9e-4	0
0	1.1e-3	1.3e-3	-1.9e-3	-2.5e-2	-4.1e-4	-2.8e-4	1.2e-4	-7.1e-4	0
0	-4.8e-4	3.9e-5	-7.6e-5	-4.1e-4	-2.5e-2	-1.6e-3	-1.9e-3	1.4e-3	0
0	-1.1e-3	-3.8e-4	1.2e-3	-2.8e-4	-1.6e-3	-2.8e-2	6.2e-4	-2.7e-3	0
0	1.3e-3	6.4e-4	2.7e-4	1.2e-4	-1.9e-3	6.2e-4	-3.0e-2	-2.8e-4	0
0	-8.0e-5	-1.2e-3	-9.9e-4	-7.1e-4	1.4e-3	-2.7e-3	-2.8e-4	-2.9e-2	0
0	0	0	0	0	0	0	0	0	0

2.3.4 Relations between residues

For lossless ideal case, the residues of realizable network must satisfy the rules in (2.6). When the circuit is lossless, the relations need to be modified. Poles of the admittance parameters are the roots of the denominator which is derived from S parameters.

$$Y_d = (1 + S_{11}) \cdot (1 + S_{22}) - S_{12} \cdot S_{21} = 0 \tag{2.27}$$

At each pole, the numerators of the Y parameters can be simplified as

$$Y_{11n} = (1 - S_{11}) \cdot (1 + S_{22}) - S_{12} \cdot S_{21} = 2(1 + S_{22}) \tag{1.28}$$

$$Y_{22n} = (1 + S_{11}) \cdot (1 - S_{22}) - S_{12} \cdot S_{21} = 2(1 + S_{11}) \tag{1.29}$$

$$Y_{21n} = 2S_{21} \tag{1.30}$$

Because the residues are positively proportional to the value of numerator of Y, we have following relation for the kth term of the partial expansion of Y parameters

$$r_{11}(k) r_{22}(k) = r_{21}^2(k) \tag{1.31}$$

When the circuit is lossy, (2.31) needs to be revised. At each pole, because of the existence of dissipation factor, the denominator of Y parameters can not reach to zero at a real frequency but have a very small positive value.

$$Y_d = (1 + S_{11}) \cdot (1 + S_{22}) - S_{12} \cdot S_{21} = \delta \tag{1.32}$$

So the relation in (1.29) is only satisfied with a small tolerance relating to loss.

2.4 CASE OF DEGENERATED POLES

For a filter of a high order degree, it is frequently seen that two or more poles of the Y parameters are located so close to each other such that only one 'peak' is shown. This problem is more severe in diagnosing a high order lossy filter. An 8[th] degree filter with its known coupling matrix is used as an example to illustrate the problem. In Fig.6, two sets of Y_{11} are plotted using absolute values. The first set is lossless and the second one is lossy with Qu equals 8000 for each cavity. As one can see in the figure when there is loss, the magnitude of poles of Y parameters will be reduced. When two poles are close to each other which is usually a case for a high order filter, the decreased poles may merge into each other in the plot. As a result, only one pole is detected and this is called degenerated pole.

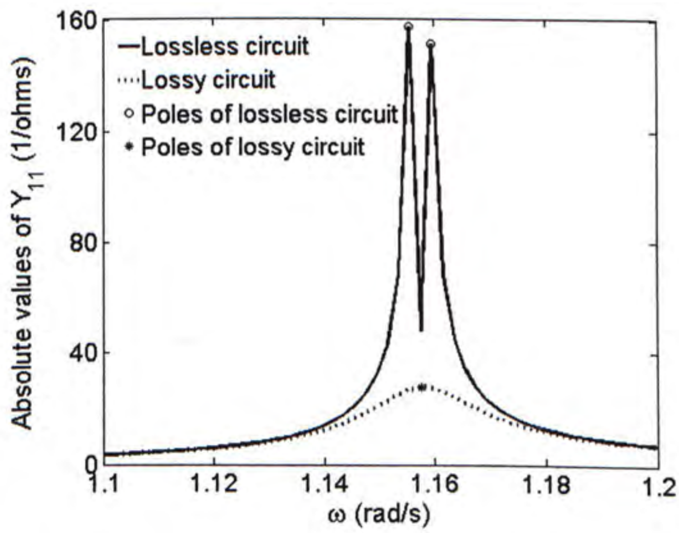

Fig. 2.7: The plot of the poles of Y11 using lossless and lossy circuit model.

2.4.1 The determination of poles

Since the proposed method for coupling matrix extraction is based on the identification of poles, for the pole degenerated case, the first step is to determine those poles disappeared because of loss. When the rational polynomials approximation of the Y parameters is accurate, poles can be found by solving the roots of the denominator polynomial. To do that, different algorithms are used to find the denominator polynomial from the measured data.

Y parameters interpolation method

In the following section, the Thiele's continued fraction algorithm [17] is used to determine the rational interpolation of Y parameters. The question is for a set of x_i and a set of f_i , find a rational polynomial ϕ_n^n,so that $\phi_n^n(x_i)=f_i$. A summary of the algorithm is listed below.

Thiele's continued fraction is

$$\phi_n^n(x) = f_0 + \cfrac{x - x_0}{\rho(x_0, x_1) + \cfrac{x - x_1}{\rho(x_0, x_1, x_2) - \rho(x_0) + .. + \cfrac{x - x_{2n-1}}{\rho(x_0, .., x_{2n}) - \rho(x_0, .., x_{2n-2})}}} \tag{2.33}$$

where the degrees of numerator and denominator are increased one by one

$$\begin{aligned} \rho(x_i) &= f_i \\ \rho(x_i, x_k) &= \frac{x_i - x_k}{f_i - f_k} \\ \rho(x_i, x_{i+1}, \ldots\ldots, x_{i+k}) &= \frac{x_i - x_{i+k}}{\rho(x_i, \ldots\ldots, x_{i+k-1}) - \rho(x_{i+1}, \ldots\ldots, x_{i+k})} \end{aligned} \tag{2.34}$$

and ρ is reciprocal difference and can be arranged in the tableau for calculation.

$$
\begin{array}{c|ccccccc}
x_0 & f_0 & & & & & \\
 & & \rho(x_0,x_1) & & & & \\
x_1 & f_1 & & \rho(x_0,x_1,x_2) & & & \\
 & & \rho(x_1,x_2) & & \rho(x_0,x_1,x_2,x_3) & & \\
x_2 & f_2 & & \rho(x_1,x_2,x_3) & & & \\
 & & \rho(x_2,x_3) & & & & \\
x_3 & f_3 & & & & &
\end{array}
\tag{2.35}
$$

This method is similar to Stoer-Bulirsch interpolation [17]. The difference is that Stoer-Bulirsch interpolation finds the interpolated value for a given x, while this method find a rational polynomial, so that poles of Y_{11} can be found by solving for roots of the denominator of interpolated polynomial.

Using the poles found by this method, coupling matrix extraction procedure can be continued. The comparison between measurement and extraction are shown in Table 4.

Table 4: Poles and Qu extracted using interpolation

Pole		Qu	
Ideal	Extracted	Ideal	Extracted
1.1577	1.1589	8000	8000
1.1557	1.1571	8000	8000
0.9371	0.93928	8000	8000
0.5578	0.5586	8000	7990
0.0134	0.0142	8000	8010
-0.5388	0.53791	8000	8050
-1.0789	-1.0779	8000	7990
-1.2837	-1.2831	8000	8000

This method is very accurate for most of the cases. But this interpolation method can not deal with high level of noise in the measured data. Besides, the number of sampling is defined for a given filter order, the sampling frequencies need to be chosen carefully. From our experience, it is better to include the poles into the samples. For practical usage, this method is in the final stage of tuning with a narrow range of data when all the poles are near to the required position.

Interpolation of denominator of Y parameter

The denominator of Y parameters derived from S parameters can be expressed by a rational polynomial (2.36). The poles of the Y parameters are the roots of the numerator of Y_d.

$$Y_d = (1 + S_{11}) \cdot (1 + S_{22}) - S_{12} \cdot S_{21} \tag{2.36}$$

Padé approximation [18] is applied to fit the polynomial Y_d, and then poles are calculated as the zeros of this polynomial. Since the denominator in the expression of (2.36) is actually the E polynomial used filter synthesis which has no poles near the imaginary axis $j\omega$, the accuracy of the fitting of denominator using rational polynomial can be guaranteed. Using the same 8^{th} degree example, the fitting of Yd and the poles solved are shown in Fig. 2.8 and the extracted elements are listed in Table 5.

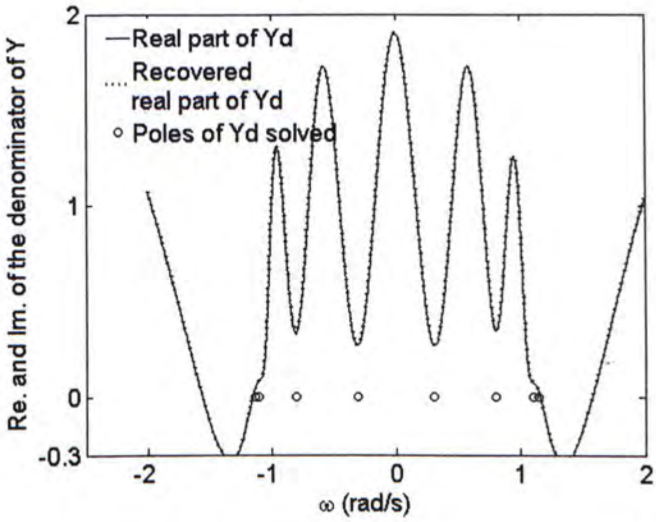

Fig. 2.8: Circuit model of a lossy 8 degree filter showing the fitted Yd and pole

Table 5: Poles and Qu extracted using Padé approximation comparing to template.

Pole		Qu	
Ideal	Extracted	Ideal	Extracted
1.1577	1.1583	8000	8000
1.1557	1.1568	8000	7990
0.9371	0.9393	8000	7880
0.5578	0.5586	8000	7790
0.0134	0.0142	8000	8300
-0.5388	0.5379	8000	8050
-1.0789	-1.0779	8000	7930
-1.2837	-1.2831	8000	7970

Just by comparing the values of Table 4 and Table 5, one may conclude that this method is not as accurate as the Y parameter interpolation method. But since the interpolation method uses least square algorithm, it can be applied to a lossy case. Also, the number and distribution of sampling frequencies are not strictly defined. This method can be applied to filter with detuned resonator.

Vector fitting method

Vector fitting method [19] can also be applied to determine the polynomial expressions of the denominator. The algorithm is summarized here for reference.

To fit a Y parameter as shown in (2.37), an unknown function σ is introduced, so that

$$Y_{11}(s)=\sum_{n=1}^{N}\frac{r_{11}(n)}{s-\lambda(n)} \tag{2.37}$$

$$\begin{aligned}\sigma(s)Y_{11}(s)&=\sum_{n=1}^{N}\frac{r_{11}(n)}{s-\overline{\lambda}(n)}\\ \sigma(s)&=\sum_{n=1}^{N}\frac{\overline{r_{11}}(n)}{s-\overline{\lambda}(n)}+1\end{aligned} \tag{2.38}$$

where $\overline{\lambda}(n)$ are the starting poles. Then

$$\sum_{n=1}^{N}\frac{r_{11}(n)}{s-\overline{\lambda}(n)}=\left(\sum_{n=1}^{N}\frac{\overline{r_{11}}(n)}{s-\overline{\lambda}(n)}+1\right)Y_{11}(s) \tag{2.39}$$

The coefficients $r_{11}(n)$ and $\overline{r}_{11}(n)$ of this expression (2.39) can be determined by least square method solving the over-determined system. The left hand side and right hand side of the above equation (2.39) can be expressed as (2.40) and (2.40) using partial expansion.

$$\sum_{n=1}^{N}\frac{r_{11}(n)}{s-\overline{\lambda}(n)}=h\frac{\prod_{n=1}^{N+1}(s-z_n)}{\prod_{n=1}^{N}(s-\overline{\lambda}(n))} \tag{2.40}$$

$$\left(\sum_{n=1}^{N}\frac{\overline{r_{11}}(n)}{s-\overline{\lambda}(n)}+1\right)=\frac{\prod_{n=1}^{N}(s-\overline{z}_n)}{\prod_{n=1}^{N}(s-\overline{\lambda}(n))} \tag{2.41}$$

So that Y_{11} can be determined by

$$Y_{11}(s)=\frac{\prod_{n=1}^{N+1}(s-Z_n)}{\prod_{n=1}^{N}(s-\overline{z}_n)} \tag{2.42}$$

Because of the embedded least square algorithm, this method can deal with loss. Also iteration process makes this method more stable.

2.4.2 The determination of residues

When the poles are not distinctive as in the pole degenerated case, the earlier procedure for determining the residues can not be applied. Since the numerator of Y parameter is a linear function of residues according to (2.9), least square method can be applied to find the residues.

For some filter responses, even when the matching of Y parameters are acceptable, the fitting to S parameters may not be successful and that is because the residues extracted do not satisfy one of the basic rules. For example when loss makes the values of poles of one of the Y parameters very small, it is difficult to accurately determine the corresponding residues. Under this condition, (2.43) shows that when the pole of Y_{11} is very small, to make the relation valid, the pole of Y_{22} must be large. Due to the facts that only two parameters from r_{11}, r_{21} and r_{22} are need to determine the CM. For example, when the value of r_{21} is very small which is shown by low magnitude of the poles of Y_{21}, Y_{11} and Y_{22} can be chosen to find the corresponding residues, then r_{21} can be found by:

$$r_{11}(k)r_{22}(k) \approx r_{11}(k)^2 \tag{2.43}$$

Using the same pole degenerated 8^{th} degree filter discussed earlier, the recovery Y_{21} is shown in Fig. 2.9. The curve 'recoverd2' represents the curve recovered using r_{21} calculated by (2.43). With an appropriate choice of the residue parameters, as shown in Fig. 2.10, the extracted S parameters for this degenerated pole case can fit the original responses very well.

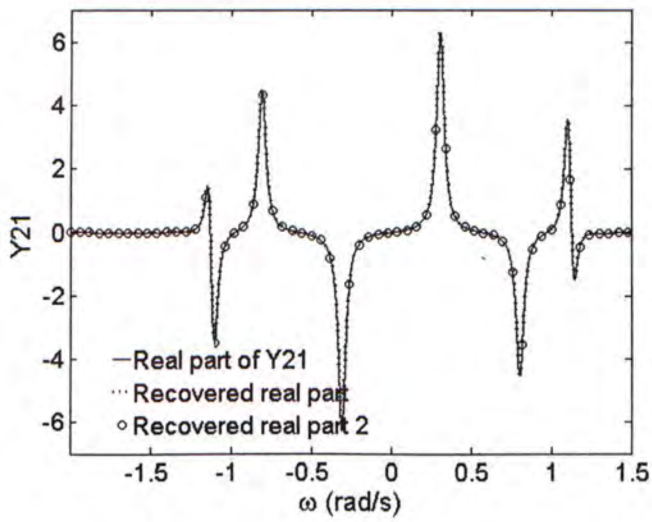

Fig. 2.9: Recovery of Y_{21} using r_{21} and r_{21_2}.

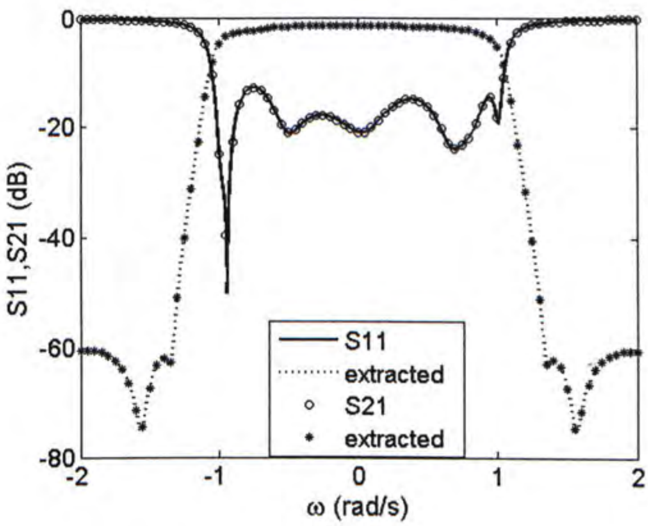

Fig. 2.10: Circuit model of a lossy 8 degree filter with S from circuit model and extraction

Chapter 3

DATA RATIONALIZATION

Engineering problems represent exercises in approximation.

— Chandra M. Kudsia

In both coupling matrix synthesis and coupling matrix extraction, we have an assumption that the physically realized filter can be represented by a rational modal. The characteristics of a general Chebyshev filter can be represented by a circuit model of inter-coupled resonators whose transfer and reflection functions can be characterized by a set of rational polynomials. In a circuit model, the input/output (I/O) couplings are represented by a simple inverter without any embedded transmission lines at I/O ports (a shift of reference planes). In a physical model, however, the scenario is no longer the same due to the existence of two non-ideal effects:

(1) a length of transmission line connecting to the I/O inverters of the filter, which contributes a frequency dependent phase term.

(2) a phase loading at I/O ports caused by the stored energy at the vicinity of I/O coupling structures. The phase loading is a constant difference between the phases of the reflection coefficients of the circuit model and those of the physical model. The phase loading is only determined by the I/O coupling structure and its immediately associated resonator.

3.1 QUASI-SB-AFS INTERPOLATION

A quasi adaptive frequency sampling with Stoer-Bulirsch algorithm is applied to the measured data in this work before conducting rational interpolation. Comparing to the SB-AFS in [20], the testing points are the measured points and the samplings are also chosen among the measured data. The procedure begins with two measured points that are at the edge of desired frequency band. The next sampling point used in the iteration procedure, which has to be chosen among the measured data, is the one with maximum interpolation error. The iteration continues until the interpolation error meets our requirement. We define the interpolation error as the absolute distance between each interpolated data and measured data. There three benefits of using this method:

(1). To remove the measurement noise. The interpolated data guarantees our measured data can be modeled by rational functions.

(2). To increase the accuracy of the numerical values of poles. Since this algorithm can predict circuit response of any accuracy with given samples, the accuracy of coupling matrix extraction is improved due to the accurate determination of the positions of poles.

(3). To reduce the time for getting S parameters from network analyzer. Typically, for S parameters of an EM model, only 14 sampling frequencies are needed to make the error of SB-AFS reasonable. For real time measurement, because of the existence of measurement noise, the number of sampling will be larger. For a 10^{th} degree filter, 30 samples are usually needed.

3.2 REMOVAL OF PHASE LOADING

Phase loading is a parameter first introduced in [11]. In this thesis, it is proved that phase loading a frequency-invariant shift between circuit model and physical filter. A method for removing phase loading is presented by analyzing the basic properties of a circuit model. The concept we are trying to emphasize here is that the phases of the S parameters of measured data which is usually neglected earlier have great impact on coupling matrix extraction. A rational model which is represented by a coupling matrix can be derived only when phase loading is removed properly. Then, the eigenvalues of the network can be found as the positions of the poles of the Y parameters thus the number of variables need for the extraction is reduced.

3.2.1 Single cavity measurement method

To justify the existence of a phase loading, the reflection coefficients of a lossy single resonator with an I/O coupling is examined first. The physical model is a full-wave EM simulation of a circular waveguide resonator with a rectangular input coupling iris and a WR75 interfacing waveguide. When the first cavity is detached, only one resonant can be observed.

It can be shown that group delay and external Q are related by

$$\tau = -\frac{\partial \phi}{\partial \omega}\text{ , and } Q_e = \frac{\omega_0 \tau}{4} \tag{3.1}$$

So the input coupling can be found by group delay as

$$R_s = \frac{f_0}{Q_e \cdot BW} = \frac{2}{\pi \tau \cdot BW}\text{ , and } M_{01} = \sqrt{R_s} \tag{3.2}$$

A circuit model is then designed such that its input coupling value and the resonant frequency are the same as those of the physical model. With the filter's bandwidth and center frequency, the value of M_{01} coupling can be calculated by the group delay of EM model. The circuit modal is used to show the ideal phase of this cavity without phase loading.

A comparison between the reflection coefficients of the two models is shown in Fig. 3.0. In order to identify the resonant frequency, a certain amount of loss is introduced in the two models. It can be seen that the phases of the two models match each other only after the phase loading of 148° is subtracted from the physical model.

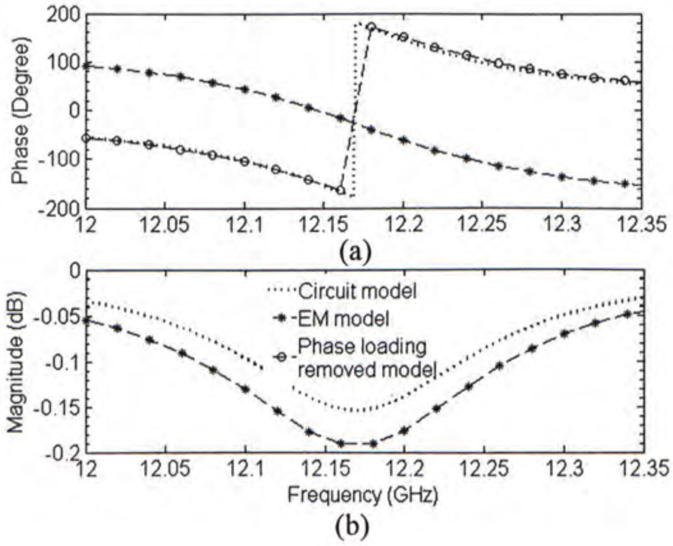

Fig. 3.0: (a) The phases and (b) amplitudes of S_{11} of EM simulated and a circuit model for a single cavity resonator with resonant frequency of 12.17GHz.

By this example, we can make the conclusion that phase loading has in fact a constant value which can be determined and removed by using single cavity. This method is accurate, but difficult to implement in real time application.

In fact, the existence of a phase loading has been indirectly proved by some previously proposed CAT methods. In [1, 9, 10], when determining the circuit parameters of a filter from a measured dataset, the effect of a constant phase loading is unintentionally removed by using the derivative of phases with respect to frequency. Nevertheless, in order to extract a filter coupling matrix, a systematic and legitimate treatment of removing the phase loading from a measured response needs to be developed for a general narrow band coupled resonator filter.

3.2.2 Multiple cavity measurement method

Asymptote of phase using S parameters

When S parameter is expressed in terms of rational polynomials [4] as in (3.3), there are two rules for the coefficients of the numerator and denominator polynomials.

(1) Because the zeros of E polynomial are asymmetrically located along the imaginary axes, all except the leading coefficient of E are complex.

(2) Zeros of F polynomial are distributed asymmetrically along the imaginary axes. The coefficients of F polynomial alternate between purely real and purely imaginary as the power of s increases.

$$S_{11} = F(S)\varepsilon_R / E(S) \tag{3.3}$$

where E(s) is an Nth degree polynomial with complex coefficients e_0, e_1, e_2, ... , e_N , F(s) is an Nth degree polynomial with complex coefficients f_0, f_1, f_2, ..., f_N , ε_R allows the normalization of the highest degree coefficients of E(s) and F(s) to unity, (ie, e_N and f_N = 1), S = jω and N is the degree of the filter

The phase of the reflection coefficient can be expressed as:

$$\phi_{S_{11}} = \tan^{-1} \frac{e_{(n-1),r}\omega^{n-1} + e_{(n-2),i}\omega^{n-2} + \ldots + e_{0,i}}{\omega^n + e_{(n-1),i}\omega^{n-1} + \ldots + e_{0,r}} \tag{3.4}$$

Therefore, as $\omega \to \pm\infty$, the phase of S_{11} can be approximated as

$$\begin{aligned} \phi_{S_{11}} &= \tan^{-1} \frac{e_{(n-1),r}\omega^{-1} + e_{(n-2),i}\omega^{-2} + \ldots + e_{0,i}\omega^{-n}}{1 + e_{(n-1),i}\omega^{-2} + \ldots + e_{0,r}\omega^{-n}} \\ &\approx \tan^{-1} \frac{e_{(n-1),r}}{\omega} \approx \frac{a_1}{\omega} \end{aligned} \tag{3.5}$$

So the group delay of S_{11} can be expressed as

$$
\begin{aligned}
\tau_{S_{11}} &= \frac{\partial \phi_{S_{11}}}{\partial \omega_b} = \frac{\partial (a/\omega)}{\partial \omega_b} = \frac{\partial \left(\dfrac{a_1}{\dfrac{f_0}{BW}\left(\dfrac{\omega_b}{\omega_0} - \dfrac{\omega_0}{\omega_b}\right)} \right)}{\partial \omega_b} \\
&= -\frac{a_1 \cdot BW}{f_0} \cdot \frac{1}{\left(\dfrac{\omega_b}{\omega_0} - \dfrac{\omega_0}{\omega_b} \right)^2} \cdot \left(\frac{1}{\omega_0} + \frac{\omega_0}{\omega_b^2} \right) \\
&= \frac{-a_1 \dfrac{f_0}{BW}\left(\dfrac{1}{\omega_0} + \dfrac{\omega_0}{\omega_b^2} \right)}{\left(\dfrac{f_0}{BW}\left(\dfrac{\omega_b}{\omega_0} - \dfrac{\omega_0}{\omega_b}\right) \right)^2} = \frac{-\dfrac{a_1}{2\pi BW}\left(1 + \dfrac{\omega_0^2}{\omega_b^2} \right)}{\left(\dfrac{f_0}{BW}\left(\dfrac{\omega_b}{\omega_0} - \dfrac{\omega_0}{\omega_b}\right) \right)^2} \\
&= \frac{-\dfrac{a_1}{2\pi BW}\left(1 + \left(\dfrac{\omega_0}{\omega_0 \pm nBW} \right)^2 \right)}{\left(\dfrac{f_0}{BW}\left(\dfrac{\omega_b}{\omega_0} - \dfrac{\omega_0}{\omega_b}\right) \right)^2} = \frac{-\dfrac{a_1}{2\pi BW}\left(1 + \left(1 \mp \dfrac{nBW}{\omega_0 \pm nBW} \right)^2 \right)}{\left(\dfrac{f_0}{BW}\left(\dfrac{\omega_b}{\omega_0} - \dfrac{\omega_0}{\omega_b}\right) \right)^2}
\end{aligned}
\tag{3.6}
$$

For narrow band Chebyshev filter, the fractional bandwidth is typically 2%. Since n is always chosen as 2 or 3

$$
\frac{nBW}{\omega_b} \approx 0 \tag{3.7}
$$

Using band pass to lowpass transformation again, the asymptote of group delay can be approximated as

$$
\tau_{S_{11}} \approx -\frac{a_2}{\omega^2} \tag{3.8}
$$

Asymptote of phase using low-pass circuit model

The transversal circuit model [4] of an Nth degree filter is shown in Fig. 3.1. The circuit model consists of N sub-networks and each of them containing two admittance inverters one frequency invariant reactance and one capacitance.

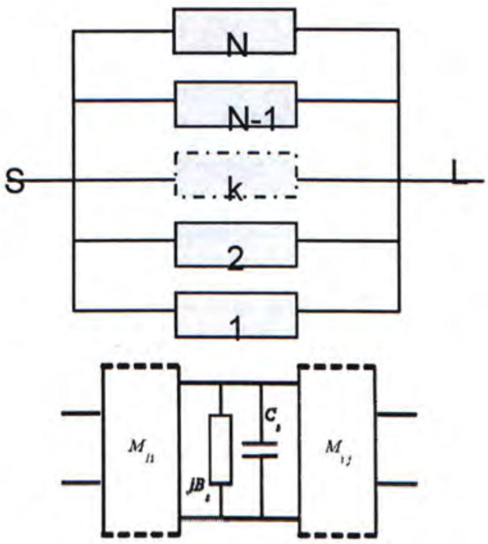

Fig. 3.1: Circuit model for transversal array.

The short circuit admittance parameters of the entire network can be derived using those elements as

$$
\begin{aligned}
Y_{11} &= -j\sum_{i=1}^{n}\frac{M_{si}^2}{\omega C_i + B_i} \\
Y_{21} &= -j\sum_{i=1}^{n}\frac{M_{si}M_{Li}}{\omega C_i + B_i} \\
Y_{22} &= -j\sum_{i=1}^{n}\frac{M_{Li}^2}{\omega C_i + B_i}
\end{aligned}
\tag{3.9}
$$

Then S parameters can be expressed though a standard parameter transformation as

$$S_{11} = \frac{(1-Y_{11})(1+Y_{22})+Y_{12}Y_{21}}{(1+Y_{11})(1+Y_{22})-Y_{12}Y_{21}}$$

$$= \frac{(1+j\sum_{i=1}^{n}\frac{M_{si}^2}{\omega C_i + B_i})(1-j\sum_{i=1}^{n}\frac{M_{Li}^2}{\omega C_i + B_i}) - \left(\sum_{i=1}^{n}\frac{M_{si}M_{Li}}{\omega C_i + B_i}\right)^2}{(1-j\sum_{i=1}^{n}\frac{M_{si}^2}{\omega C_i + B_i})(1-j\sum_{i=1}^{n}\frac{M_{Li}^2}{\omega C_i + B_i}) + \left(\sum_{i=1}^{n}\frac{M_{si}M_{Li}}{\omega C_i + B_i}\right)^2} \tag{3.10}$$

When $\omega \to \pm\infty$, the first order approximation of S11 is

$$S_{11} \approx \frac{(1+j\sum_{i=1}^{n}\frac{M_{si}^2}{\omega C_i + B_i})}{(1-j\sum_{i=1}^{n}\frac{M_{si}^2}{\omega C_i + B_i})} \approx \frac{(1+j\sum_{i=1}^{n}\frac{M_{si}^2}{\omega C_i})}{(1-j\sum_{i=1}^{n}\frac{M_{si}^2}{\omega C_i})} \tag{3.11}$$

Therefore the phase of S_{11} is approximated by (3.12), and the same conclusion as (3.5) can be drawn.

$$\phi_{S_{11}} = -2\tan^{-1}\frac{X}{\omega} \propto \frac{a_1}{\omega} \tag{3.12}$$

Fig. 3.2 shows the phase and the group delay of a 4 pole band pass filter using the circuit model at the far low end frequencies. It can be seen that the phase and the group delay can be fitted very well by (3.5) and (3.8), respectively.

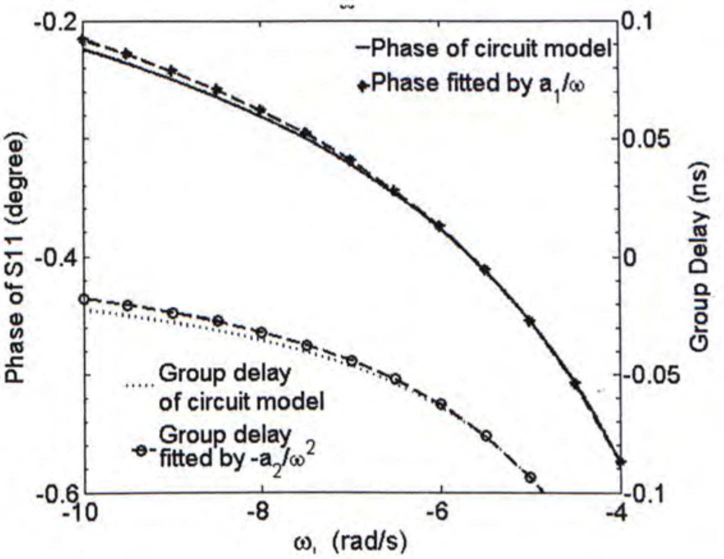

Fig. 3.2: The phase and group delay of lowpass prototype of a typical 4 pole bandpass filter at the far low end frequencies and their rational function fitting.

Method of phase loading removal

Relation (3.5) reveals that the asymptote of the phase of S_{11} outside of the pass band approaches to zero symmetrically from negative and positive sides. This fact suggests that the phase loading can be determined by finding the phase difference at two symmetric frequency points that are a few fold of bandwidth away from the center frequency, say $\omega = \pm 4$ (rad/s) in the low pass domain. The concept of the phase loading can be further illustrated by a simple filter example. Fig. 3.3 shows the phase responses of a typical 4-2 waveguide dual-mode filter obtained by an EM simulation. The original phase and the one with 127° phase loading removed are shown, illustrating the asymptotic behavior of the S_{11} phase of a physical model after removing the phase loading. The frequency variable has been transformed to its low pass domain in order to view the respective limits of the asymptote.

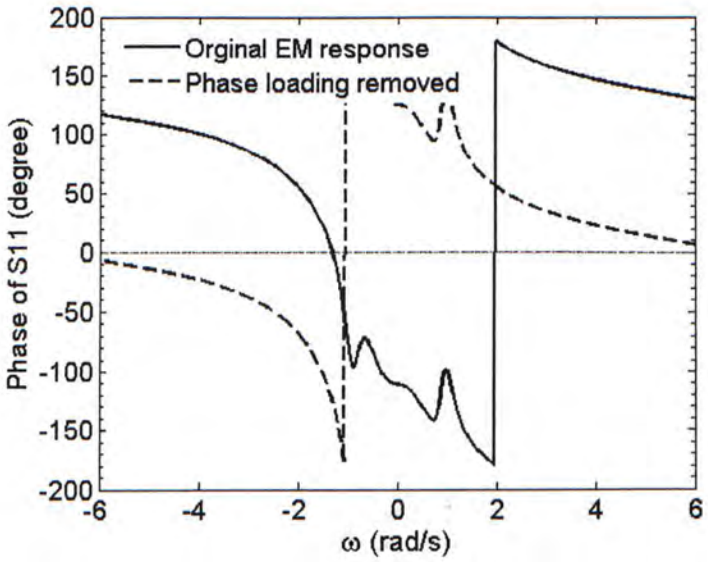

Fig. 3.3: The phases of a typical 4th degree filter with and without removing the phase loading.

The phase loading is removed by comparing the phase shift at two symmetric positions out of the pass band. This part is important in the coupling matrix extraction because it's the main reason of pole's displacement and disappearance and it guarantees that the measured data can be expressed by a proper rational modal.

The origin of phase loading may be: (1) Part of a small length of transmission line or waveguide. When the bandwidth we are considering is narrow, the effect of a small length of transmission line on S_{11} is, approximately, a constant phase shift. In optimization, phase loading is partially compensated by optimizing the length of transmission line at the input and output ports; (2) Stored static energy of higher order modes. Even though there is no extra transmission line connected to the filter, phase loading can still be observed.

3.3 DE-EMBEDDING OF THE REFERENCE PLANE

In real-time measurement, there are always transmission lines or waveguides connecting to the calibrated reference plane and the input and output ports of the filter. The length of this kind of line is sometimes difficult to measure because of the existence of higher order modes at the discontinuities. In this section, a practical way will be provided for removing the influence of waveguide or transmission line and for determining the corresponding electric length.

The method is based on the properties of the circuit model of a Chebyshev filter we derived in the last session. The effect of waveguide is approximated to a simple expression. Since measured response is the combination of the filter itself and the waveguide, the goal is to determine the response of the filter using measured data by de-embedding.

The effect of rectangular waveguide

In many waveguide filter applications, the working frequency is much larger than the cutoff frequency. When wave number k is much larger than the cutoff wave number kc, the propagation constant β can be estimated by

$$\beta = \sqrt{k^2 - k_c^2} = k\sqrt{1 - (\frac{k_c}{k})^2} \approx k - \frac{k_c^2}{2k} = 2\pi\sqrt{\varepsilon\mu} f - \frac{k_c^2}{4\pi\sqrt{\varepsilon\mu}} \cdot \frac{1}{f} \tag{3.13}$$

When a waveguide with a length of Δl is connected to the input and output ports of a filter, the new S parameters along with its phase is modified as

$$\begin{aligned} S_{ij} &= S'_{ij} e^{-2j\beta\Delta l} \\ \phi_{S_{11}} &= \phi_{S'_{11}} - 2\beta\Delta l \end{aligned} \tag{3.14}$$

Therefore, in conjunction with (3.5), when the working frequency is much higher than the cutoff frequency, the phase and group delay of measured S_{11} is contributed by the circuit model itself and the waveguide as

$$\phi_{\Delta l} = -2\beta\Delta l \approx -4\pi\sqrt{\varepsilon\mu}\Delta l \cdot f - \frac{k_c^2\Delta l}{2\pi\sqrt{\varepsilon\mu}} \cdot \frac{1}{f} \tag{3.15}$$

$$\tau_{\Delta l} = \frac{\partial \phi_{\Delta l}}{\partial \omega_b} = -2\sqrt{\varepsilon\mu}\Delta l + \frac{k_c^2\Delta l}{\sqrt{\varepsilon\mu}} \cdot \frac{1}{\omega_b^2} \tag{3.16}$$

Considering a very high frequency, the second term in group delay can be neglected. So waveguide adds a constant part to the group delay. Fig. 3.4 shows the group delay of S_{11} before and after adding a length of waveguide to a 4^{th} degree filter using EM model. Different from the effect of phase loading, the shift of group delay due to the waveguide symmetric about the center frequency, so it can not be removed by the method of removing phase loading.

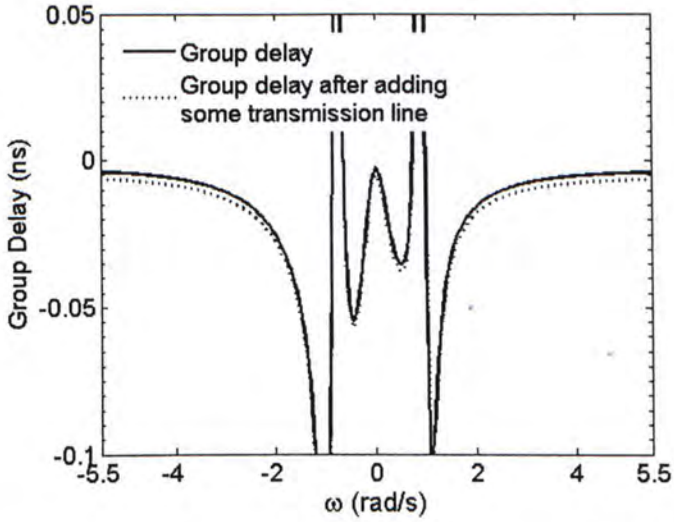

Fig. 3.4: EM simulations of group delay using 4th EM before and after adding some length of transmission line.

Methods of de-embedding

An 8th degree waveguide filter with center frequency 12GHz and bandwidth 40MHz is used here to illustrate the procedure of de-embedding. For this Ku band filter, the width of the waveguide for input and output is 0.375 inch. At center frequency, the ratio of k and kc is 1.524.

First, the accuracy of the approximation used in determining β is analyzed. Fig. 3.5 shows the β calculated using the ideal equation and the approximation. The error is about 4.0% through the pass band. One important properties of this figure is that besides the existence of a difference between the absolute values of the ideal and approximated β, the error between the slopes of these two curves is much smaller.

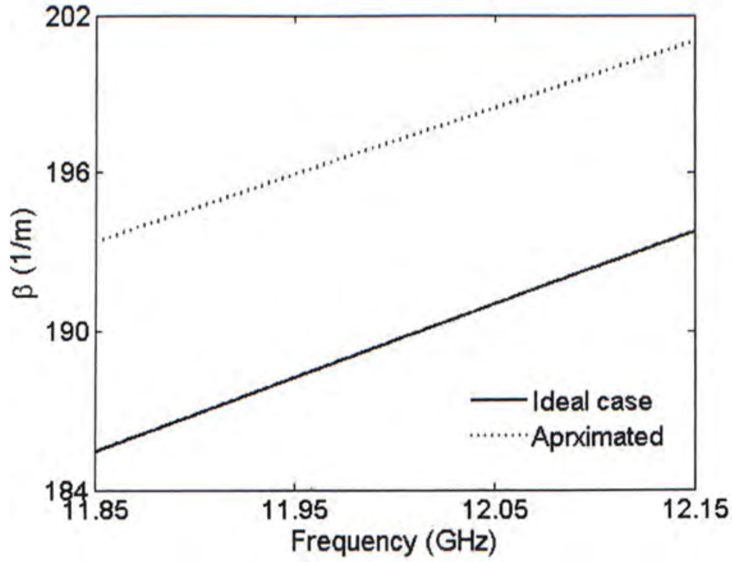

Fig. 3.5: The comparison between the ideal β and the approximated one.

From previous discussion, the group delay of measured S_{11} can be fitted to a function as (3.17), where a_2 and a_3 are two constants. The fitting range of frequency is chosen based on two rules.

(1) it should be away from filter's pass band so that the approximation on filter's phase and group delay is valid;

(2) it should not be too far away because higher order modes (spurious modes) may exist and is not practical for real-time measurement. Based on the rules, the frequency range we use is from 4 to 6 at lowpass band. Fig. 3.6 shows the fitting of the measured group delay of S_{11} using the equation. The values of a_2 and a_3 are -0.0076 and -0.4389 respectively.

$$\tau_{s11} = \frac{a_2}{\omega^2} - 2\sqrt{\varepsilon\mu}\Delta l = \frac{a_2}{\omega^2} - a_3 \tag{3.17}$$

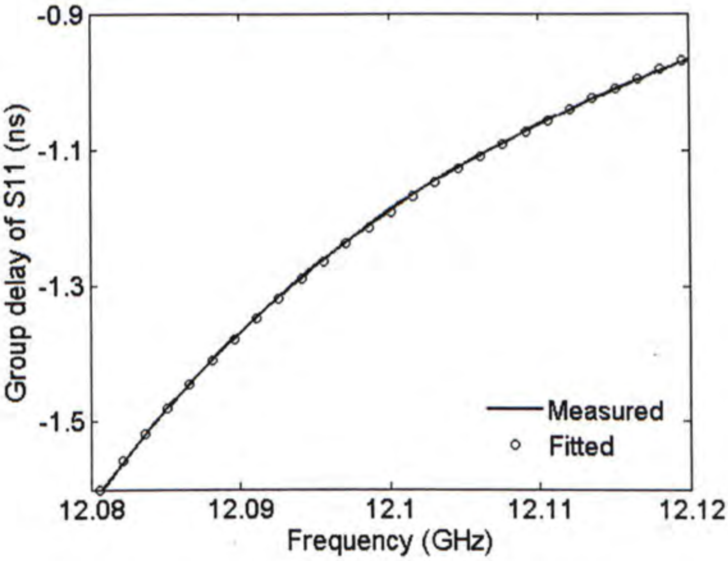

Fig. 3.6: The fitting of the group delay of S_{11}.

The constant term of group delay in the approximated expression can be determined and removed by the curve-fitting of the group delay. The parameter Δl can then be found by (3.18). Using a3 from curve fitting, the value of Δl is determined as 0.0658 m.

$$\Delta l = \frac{a_3}{-2\sqrt{\varepsilon\mu}} \tag{3.18}$$

The phase of S11 from measurement contains three parts according to (3.19), so the effects of waveguide on phase can be removed for a given Δl.

$$\phi_{S_{11}} \approx \frac{a_1}{\omega} - 2\beta\Delta l \approx \frac{a_1}{\omega} - 4\pi\sqrt{\varepsilon\mu}\Delta l \cdot f + \frac{k_c^2 \Delta l}{2\pi\sqrt{\varepsilon\mu}} \cdot \frac{1}{f} \tag{3.19}$$

Fig. 3.7 shows the phases of the 8^{th} degree filter. As one can see from the figure, the slope of the measured phase is different from the one of circuit model outside the passband. After de-embedding, the slope of the phase is corrected but a constant difference still existed but that can be removed as a phase loading. After removing phase loading of 234.7°, the phase coincides with that of the circuit model very well.

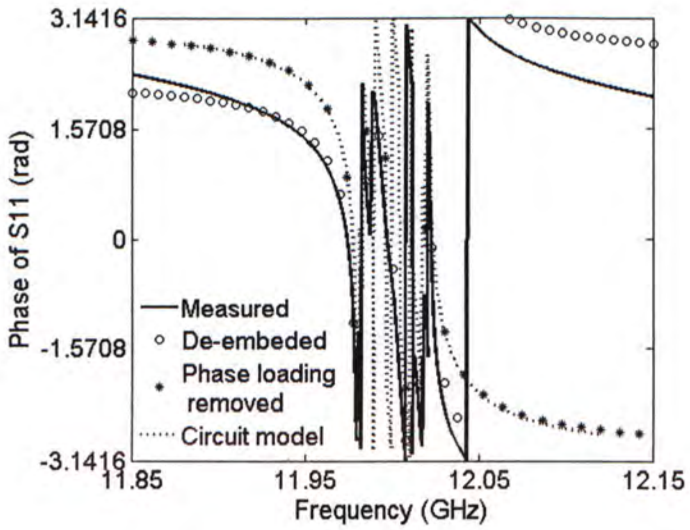

Fig. 3.7: The removing of the effect of waveguide by de-embedding and removing phase loading.

Examples of de-embedding

We test the proposed method of de-embedding by using an EM model with additional transmission lines at the input and output port, and comparing the extracted coupling matrix with the model without such addition line. The model is an 8th degree filter with center frequency 12.0 GHz and bandwidth 0.04 GHz.

Table 6: Extracted length of embedded transmission line

Embedded length (mm)	Zero	6.250	12.500	25.000	50.000
Length extracted (mm) at input port	-1.320	6.920	15.227	31.437	65.513
Length extracted (mm) at output port	-1.321	6.920	14.846	31.437	65.513
Maximum error in CM		0.0016	0.0010	0.0017	0.0012

From the example one can see that even when no additional line is added intentionally, there is still non-zero value of length from de-embedding due to discontinuity.

Fig. 3.8 shows the magnitude of Y_{11} before and after removing phase loading and de-embedding using a 4^{th} degree filter. The figure illustrates the importance of the phase of measured S parameters for the coupling matrix extraction.

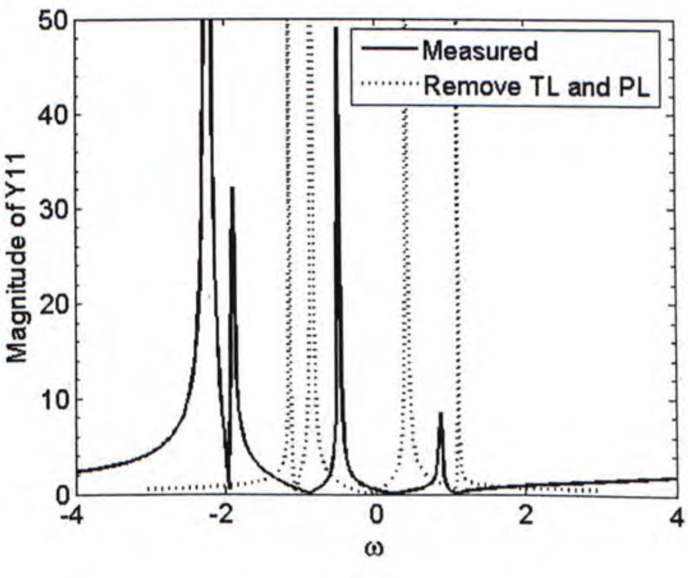

Fig. 3.8: Y parameters before and after the removing of phase loading.

Chapter 4

EXAMPLES OF COUPLING MATRIX EXTRACTION

Coupling matrix representation of microwave filter circuit is extremely useful because it is a combination of mathematical operations and real world filter properties.

— Richard J. Cameron

This chapter provides four examples of the extraction of Chebyshev narrow band filters using the software tool described in Appendix B. Besides basic procedures of coupling matrix extraction addressed in chapter 2 and 3, some practical issues are discussed here. From the author's experience, the range of data used for de-embedding is $4 \le \omega \le 6$ at lowpass band; the phase loading is removed using the data at $\omega = \pm 2.5$ of lowpass band; and the data range used for coupling matrix extraction is case-dependent.

A 4^{TH} DEGREE DR FILTER

The diagnosis of a 4-2 Ku band dielectric resonator filter with center frequency of 12.572 GHz and bandwidth of 0.04 GHz is chosen as the first example. To demonstrate the applicability of the proposed approach to a strongly de-tuned filter, one of the frequency tuning screws was strongly detuned.

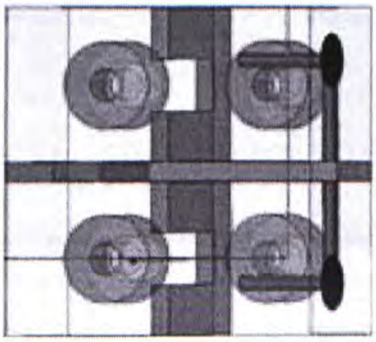

Fig. 4.0: EM model of 4th degree dielectric filter.

Fig. 4.1 shows the recovery of the admittance parameters after removing the phase loading (79.5° and 86.4° separately for input and output ports) and the embedded transmission lines (both are zero in this case). One can see from the figure that phase loading can bring serious problems because it can cause the displacement of the poles of admittance parameters. Also the filter shown is not properly tuned as one of the poles is away from the pass band with a relatively smaller magnitude.

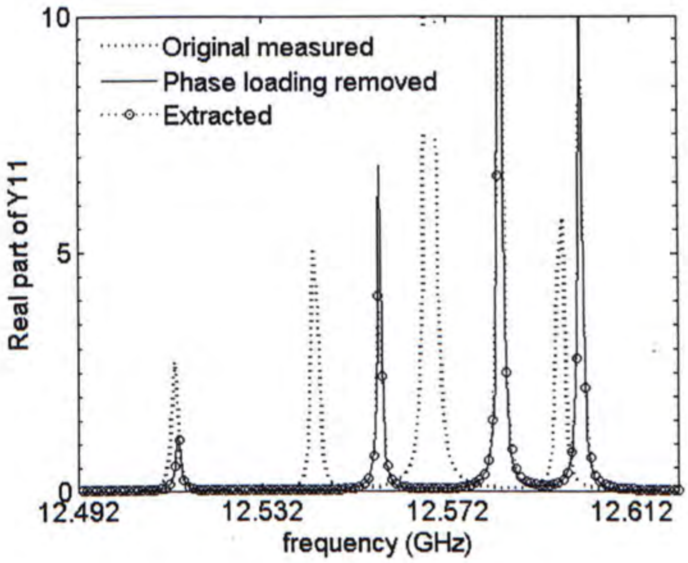

Fig. 4.1: Fitting of Y parameters using 4th degree filter.

The Fig. 4.2 shows the real and imaginary part of Y_{11}. After removing the phase loading, measured data can be represented by a circuit model and the three observations about the real and imaginary part of the admittance parameters revealed in session 1.3.1 are satisfied. One conclusion on the choice of data range for coupling matrix extraction can be drawn here that while narrow range of data make the circuit model approximation valid, the range should be wide enough to include all the poles shown in Y parameters.

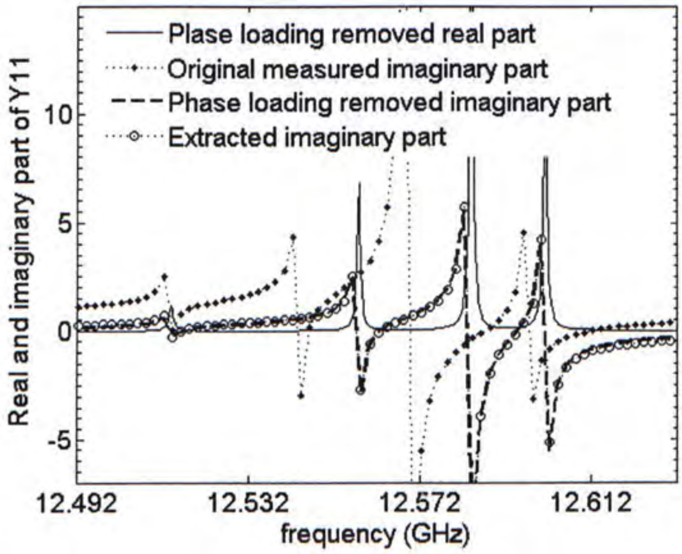

Fig. 4.2: The real part and imaginary part of Y_{11} after removing the phase loading.

In Fig.4.3, the original measured S-parameters are compared with those calculated using extracted coupling matrix. Very good agreement between these two sets of data can be observed.

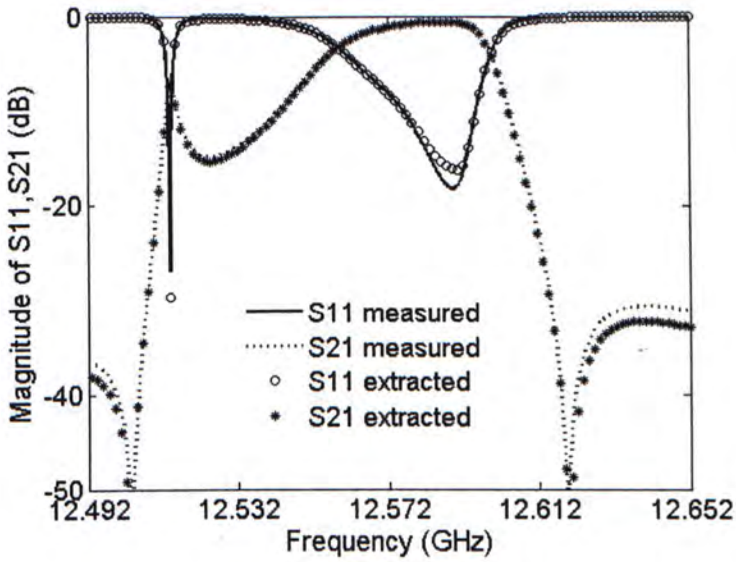

Fig. 4.3: S-parameters of a 4-2 dual model Ku band filter: the original measured and the ones from the extracted filter model.

The extracted coupling matrix is listed in Table I, in which a large M22 represents the server detuning of the second resonator. The real part of the canonical coupling matrix extracted is founded by the real part of poles and residues. After being transformed to folded structure, they represent real couplings and are shown in the first line of each cell. The elements in the second lines are real and represent loss. When loss of each resonator does not vary too much, after transformation, the diagonal elements are at least one order of magnitude larger than the off-diagonal ones. Under this condition, the loss of the entire network is mainly contributed by each individual resonator so that it can be represented by the unloaded Q of each resonator. Applying (2.13) to the diagonal elements leads to the values of unloaded Q which are13,900, 11,200, 11,700 and 14,000.

Table 7: The extracted complex matrix of the lossy 4-2 filter.

	0.9992 +0				
0.9992 +0	-0.5090 **-j2.30E-02**	-0.9536+ j8.14E-04	-j1.97E-03	-0.2140 -j1.69E-04	
	-0.9536+ j8.14E-04	1.0609 **-j2.83E-02**	1.7595+ j4.40E-03	0.2807+ -j9.23E-04	
	-j1.97E-03	1.7595+ j4.40E-03	0.9368 **-j2.72E-02**	-0.6976+ j2.56E-04	
	-0.2140 -j1.69E-04	0.2807+ -j9.23E-04	-0.6976+ j2.56E-04	0.1119 **-j2.22E-02**	1.0106 +0
				1.0106 +0	

A 6^{TH} DEGREE WAVEGUIDE FILTER

The second example is a 6^{th} degree dual-mode filter using EM model. The response is calculated using an in-house mode matching program. The conductivity of the EM model is set to be $4\times10^{7} S\cdot m^{-1}$. Phase loading of the input and output ports are 44.2° and 40.8 ° respectively. Unloaded Qs extracted are 13023, 13013, 13108, 13156, 13048 and 13062 which are quite uniform. The S parameters extracted are shown in Fig. 4.4. For filters in this typical stage, all the poles of Y parameters are already near their ideal positions of Chebyshev response, the range of data for coupling matrix extraction is set to be $-1.6 \le \omega \le 1.6$ at lowpass band.

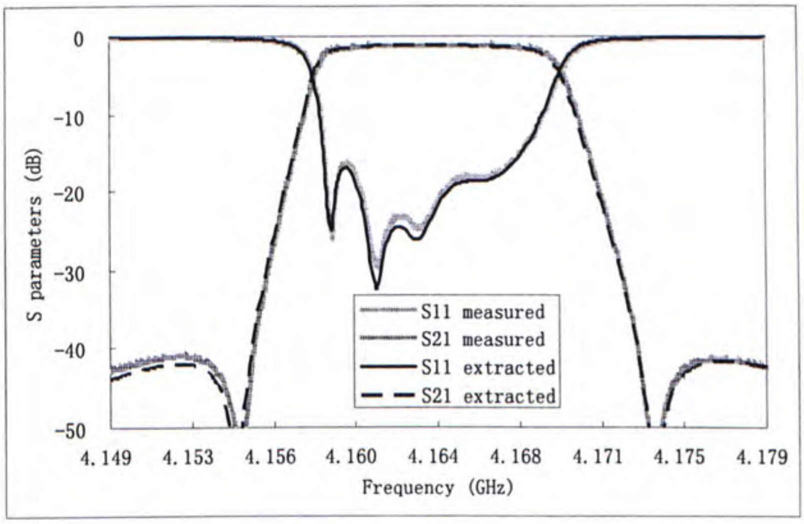

Fig. 4.4: S parameters from measurement and extraction.

AN 8^{TH} DEGREE WAVEGUIDE FILTER

This example comes from measured responses of an eighth degree Ku band dual mode circular waveguide filter with four transmission zeros. The center frequency of the filter is 11.46 GHz and the bandwidth is 0.054 GHz.

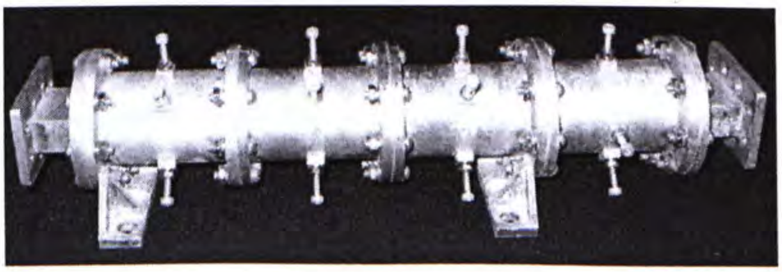

Fig. 4.5: Photo of the 8^{th} degree dual mode waveguide filter.

Phase loadings of input and output port are -72.1 ° and -76.5 ° respectively; the lengths of transmission line extracted are 99.1 mm and 94.0 mm for each port. Fig.4.6 shows the real part of Y_{11} from measurement, after the removal of the phase loading and from the extraction. The figure illustrates clearly the effect of phase loading and transmission line on shifting the poles of Y_{11}. Failing to remove the phase loading can cause the displacement of the poles' locations, thus leads to non-physical solution of the coupling matrix extraction. In another word, removing the phase loading guarantees that the measured data can be expressed by a proper rational model. In addition, as shown in the figure there are only six poles appearing. By using rational modal fitting, all eight poles can be solved. The two out most peaks consist of two poles each.

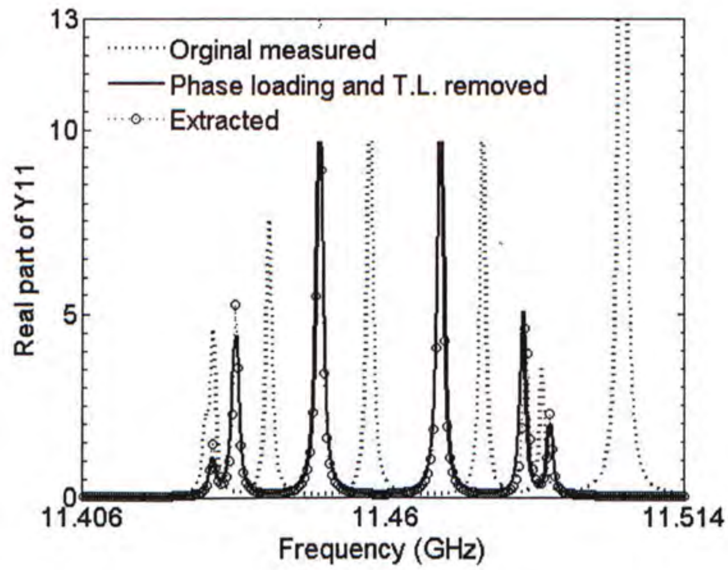

Fig. 4.6: Y parameters of the 8-4 dual mode waveguide filter.

Table 8 lists the extracted CM and Qus after transformed into the non symmetric inline configuration. Due to the limitation of the dispersion-less filter circuit model, some parasite couplings appear in the extracted CM (shown in grey numbers) to compensate the dispersion. These elements can be neglected because they are much smaller than the other elements in extracted coupling matrix.

Table 8: Extracted coupling matrix and unloaded Q

0	1.1297	0	0	0	0	0	0	0	0	Qu
1.1297	-0.0261	-0.9657	0	0.2407	0	0	0	0.0101	0.0272	1.14E+04
0	-0.9657	0.0171	-0.8138	0.0120	0	0.0090	0	-0.0250	0	1.06E+04
0	0	-0.8138	-0.0128	-0.5519	-0.0204	0	-0.0145	0	0	1.14E+04
0	0.2407	0.0120	-0.5519	0.0622	-0.5622	0.0362	0	0.0062	0	1.23E+04
0	0	0	-0.0204	-0.5622	-0.0862	-0.4015	-0.1019	-0.5303	0	1.25E+04
0	0	0.0090	0	0.0362	-0.4015	0.1594	-0.9375	0	0	1.17E+04
0	0	0	-0.0145	0	-0.1019	-0.9375	0.0053	0.8180	0	1.16E+04
0	0.0101	-0.0250	0	0.0062	-0.5303	0	0.8180	-0.0783	1.1179	1.21E+04
0	0.0272	0	0	0	0	0	0	1.1179	0	

Fig. 4.7. shows the S parameters from measurement and from the extracted coupling matrix with the parasite couplings neglected.

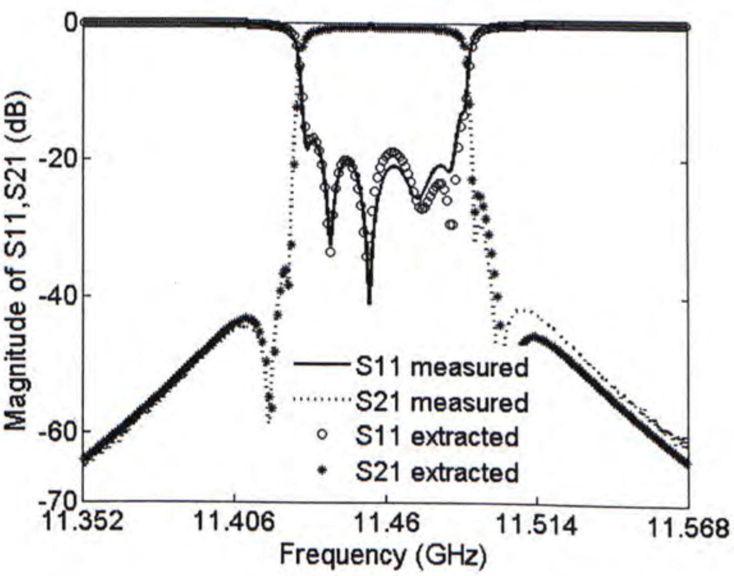

Fig. 4.7: S parameters of the 8-4 dual mode waveguide filter.

A 10^{TH} DEGREE WAVEGUIDE FILTER

This example is a 10^{th} degree dual-mode filter. The range of data used for coupling matrix extraction is an important issue for practical application. In this example, only 8 poles are shown in Fig. 4.8. Because of the high order modes, the accuracy for determining the poles has huge influence on the extraction. In order to increase the accuracy of determining the poles, the range of data used is narrower than other examples.

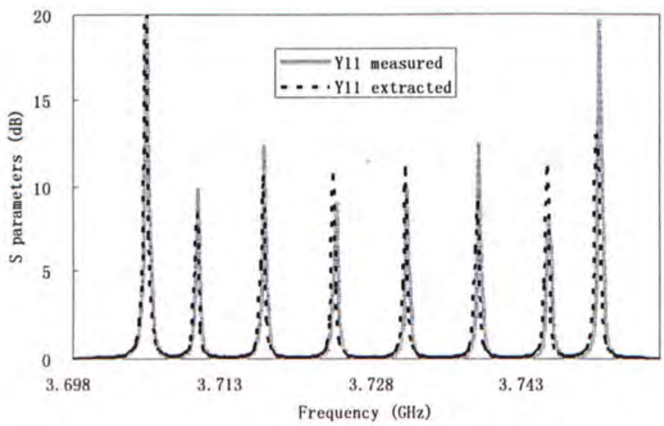

Fig. 4.8: Real part of Y_{11} of the 10th degree filter from measurement and extraction.

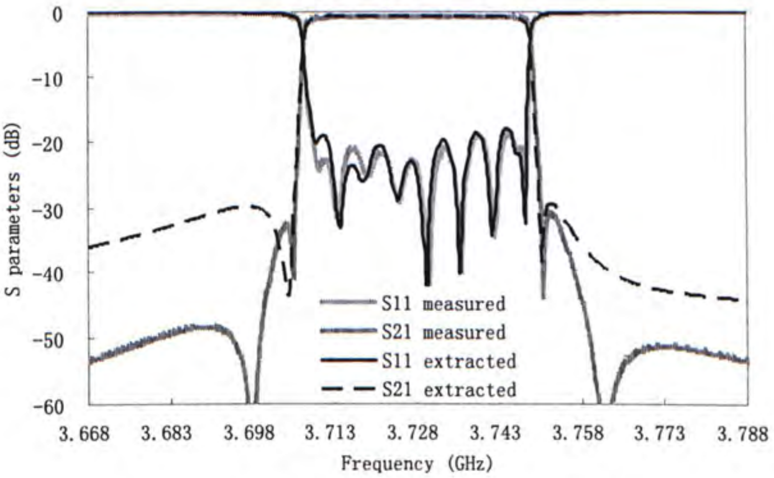

Fig. 4.9: S parameters of the 10th degree filter from measurement and extraction.

As one can see in Fig. 26, neglecting data out of passband make the outer two transmission zeros invisible for extraction, as a result the fitting of S_{21} out of the pass band is not good. But this is not a severe problem because that pair of transmission zeros is controlled by cross coupling M_{10} in folded structure. So we can adjust $M_{1,10}$ a little bit to bring the transmission zeros back and this operation do not effect the S_{11} and in-band response. After adjusting $M_{1,10}$ and setting the parasite coupling M_{1L}, $M_{2,10}$, M_{39}, M_{48} to zero, the modified response is shown in Fig. 4.10.

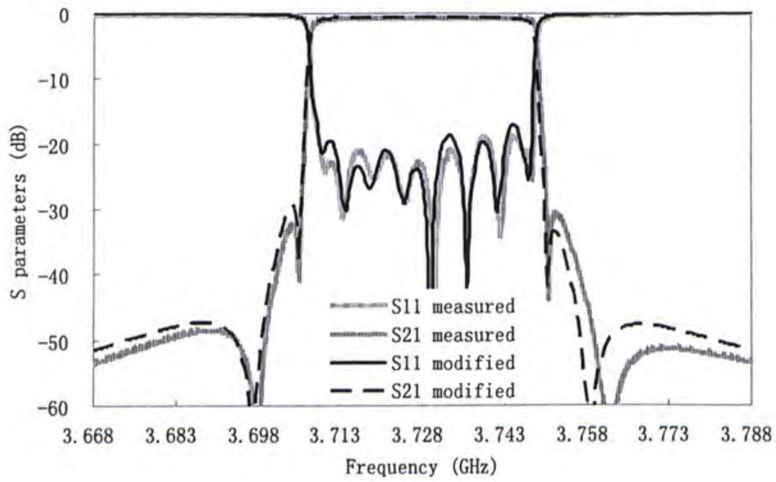

Fig. 4.10: S parameters of the 10th degree filter from measurement and from modified coupling matrix.

Chapter 5

FILTER TUNING UTILIZING COUPLING MATRIX EXTRACTION

The filter elements need tuning can be identified by a comparison between the extracted parameters which best fit the measured response and the ideal one.

— Richard J. Cameron

This chapter presents how the coupling matrix extraction method addressed in chapter 3 can be utilized in filter tuning. The first part of this chapter shows the strategies used in filters tuning utilizing coupling matrix extraction. After that, three examples of filter tuning are provided.

5.1 FILTER TUNING STRATEGIES

The derivation of coupling matrix extraction is based on the circuit model of narrow band Chebyshev filter. In the beginning, other methods such as the time domain tuning which is discussed Appendix A should be applied to bring all the poles of the Y parameter in the band of interesting.

Fig. 5.0 shows basic procedures of computer aided tuning utilizing parameter extraction. First, S parameters are obtained from network analyzer for real time measurement or from EM simulation. Coupling matrix can be extracted using an appropriate method. The differences between the extracted one and the desired one can indicate which structure in filter should be adjusted.

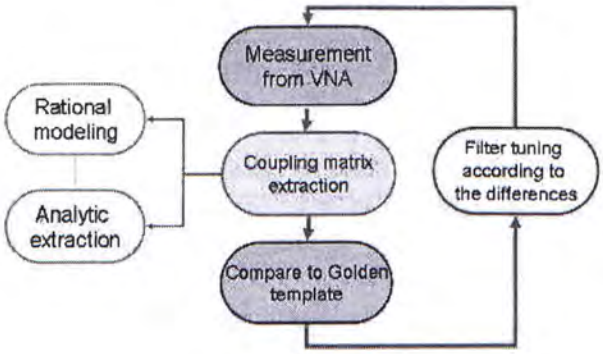

Fig. 5.0: Flow chart of filter tuning utilizing coupling matrix extraction.

Two major steps in the proposed coupling matrix extraction approach are (1) the rational modeling of measured data which includes the removing of phase loading and the de-embedding; and (2) the analytical extraction of coupling matrix, which embraces the determination of poles, residue, loss and the construction of coupling matrix with loss. Software addressed in Appendix B is designed to integrate these operations.

A filter can be tuned according to the differences between extracted coupling matrix and the designed one (golden template). In the beginning of tuning, adjustment should be applied to the element with the largest difference in coupling value. Under this strategy it is assumed that the largest difference indicates the most sensitive element. And the tuning of this particular one will make the response more similar to the one of golden template than the tuning of any other elements in coupling matrix. When the differences between the extracted coupling matrix and the template are small, or when the return loss level is below -15 dB, tuning should be applied after a sensitivity analysis which can indicate the element corresponds to the most effective change of the response.

5.2 FILTER TUNING EXAMPLES

A channel filter for multiplexer

In [21], a complete method for multiplexer syntheses is presented. Basically, coupling matrix for a channel filter is optimized such that when the filter is connected to the multiplexer, the return loss is equal ripple at the required level. As a result, response of an individual filter is with high and non-equal-ripple return loss level. Coupling matrix extraction is especially useful for tuning such 'singly terminated' filter because the tuning of such filter contradicts human experience.

Fig. 5.1 shows the phase of S_{11} during de-embedding and removing phase loading. As one can see from the figure, due to the existence of waveguide at the input port, the slope of the phase of S_{11} is nearly a constant out of the pass band. After de-embedding, the effect of waveguide with length 42 mm is eliminated from measured data, as a result, the slope of the phase is smaller. After a constant shift realized by removing phase loading, the phase is almost the same as that of the circuit model out of pass band.

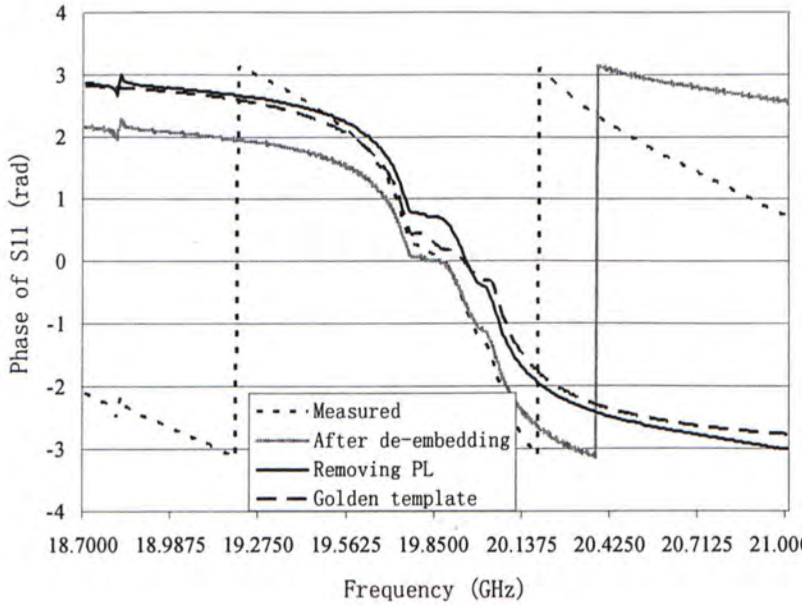

Fig. 5.1: The phase of S11 after data modification

Fig. 5.2 shows the S parameters of one channel filter from template and measurement after tuning using the coupling matrix extraction approach.

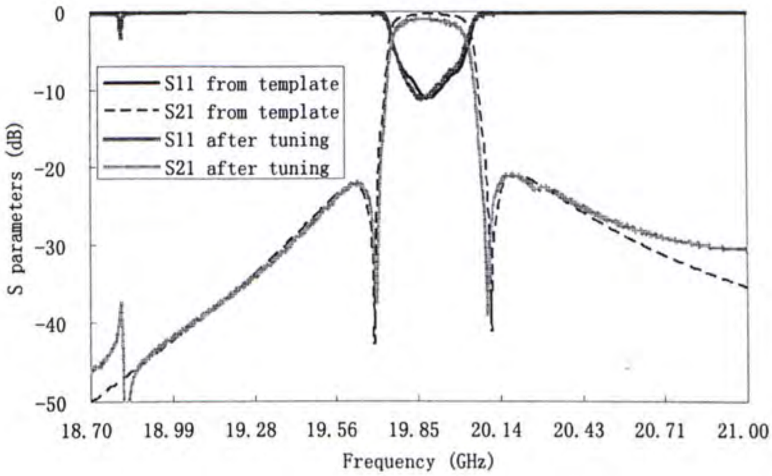

Fig. 5.2: The measured S parameters after the tuning of 4th degree channel filter.

An 8^{th} dual mode filter

In the following example, an 8^{th} degree dual mode filter with center frequency 12.45 GHz and Bandwidth 0.058 GHz is used. In the beginning the filter is pre-tuned and the coupling matrix is extracted. Then all the resonators are detuned and all the cross couplings are changed. The purpose of this example is to recover the original response using the earlier extracted coupling matrix as golden template. Fig.5.3 shows the comparison between the original response and the recovered one.

This example shows the potential of coupling matrix extraction in filter cloning for special applications.

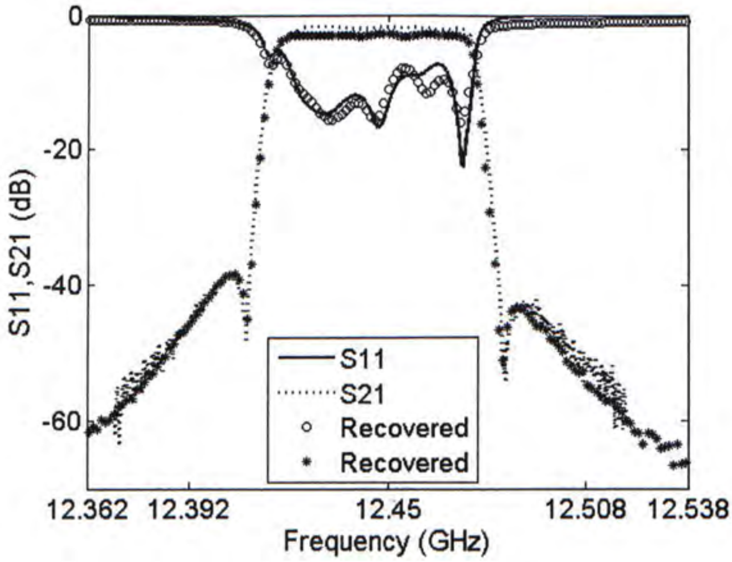

Fig. 5.3: The original and recovered S parameters.

An EM design of an 8^{th} degree dual mode filter

This example concerns with the design of an equal-ripple 8 pole dual mode circular waveguide filter. The filter response by a full-wave mode matching based electromagnetic simulation is used as the physical model as show in Fig.5.4. The center frequency of the filter is 12.0 GHz and the bandwidth is 0.05 GHz. In order to study the proposed approach for a lossy filter, the conductivity of the metal is set to 4.0×10^7 in the setting of the EM model.

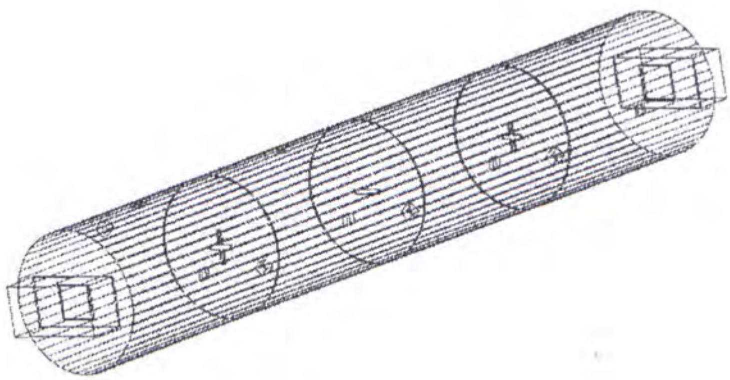

Fig. 5.4: The EM model of the 8th degree filter.

In each step of tuning, the characteristics of a filter are interpreted by a coupling matrix. Then the difference between the extracted coupling matrix and the golden template can guide the process of tuning. For most of the cases, adjustments to the resonators or couplings should be made to the element with the maximum difference. When the return loss level is lower than -17dB, that is when the maximum difference between the extracted coupling matrix and golden template is around 0.01, a sensitivity analysis should be conducted and all the elements in the extracted coupling matrix should be done first in order to find a proper element to be tuned in the next step. In this way, the tuning utilizing coupling matrix extraction can be applied until desired response has been achieved.

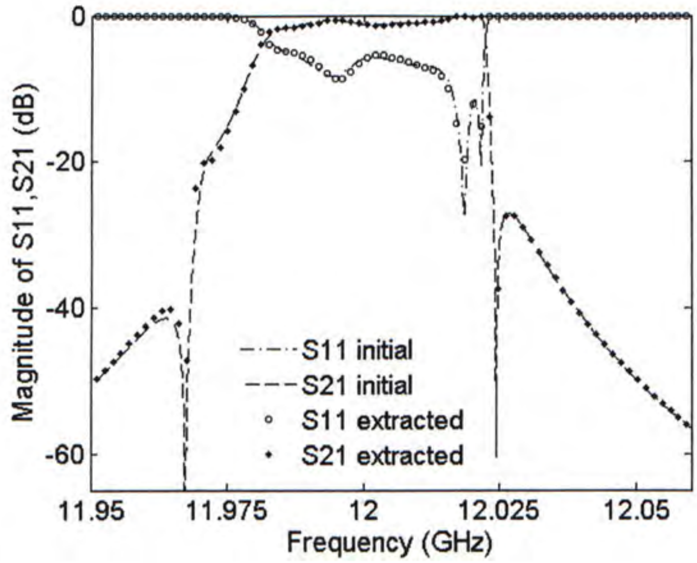

Fig. 5.5: The measured initial S parameters and their extractions of the 8-2 filter using EM simulation.

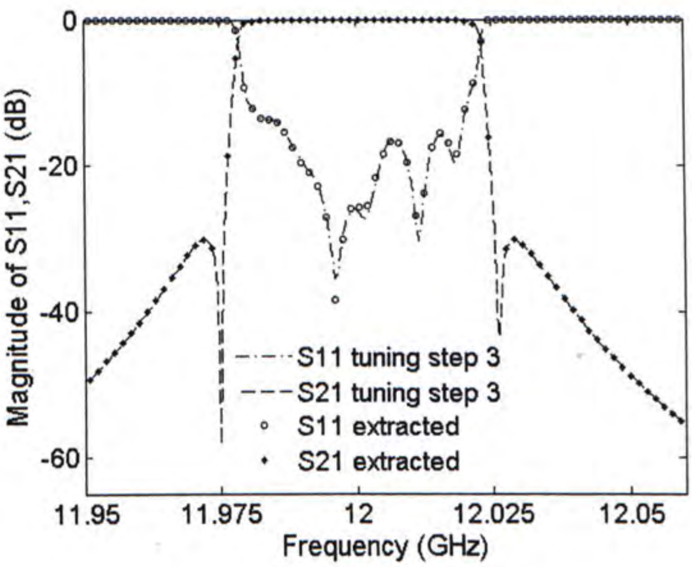

Fig. 5.6: The measured and extracted S parameters after 3 steps of tuning.

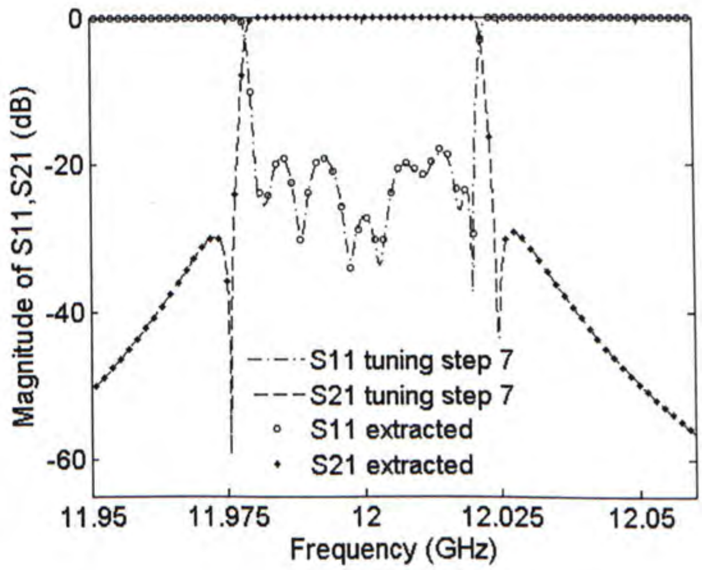

Fig. 5.7: The measured and extracted S parameters after 7 steps of tuning.

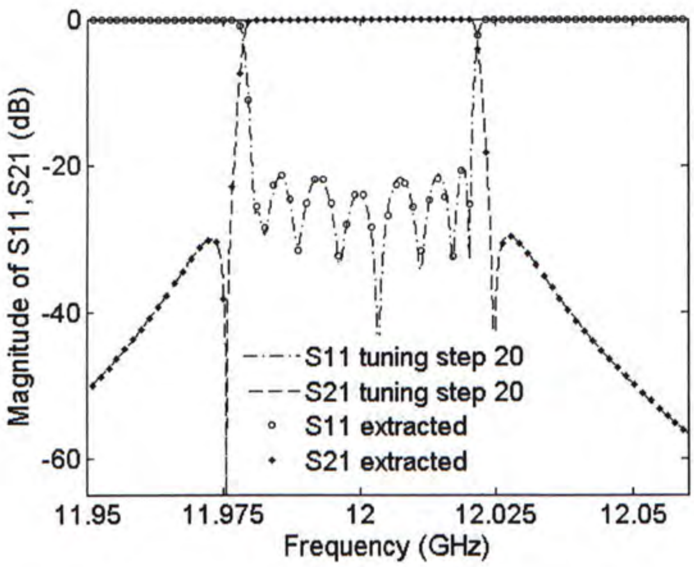

Fig. 5.8: The measured and extracted S parameters after 20 steps of tuning.

Table 9: Tuning steps of the 8^{th} degree filter

	Step 1	Step 3	Step 7	Step 20
M11	-0.0389	0.0074	0.0076	0.0104
M22	-0.1235	0.0009	-0.0011	0.0018
M33	-0.1984	-0.0217	-0.0081	-0.0009
M44	-0.0343	-0.0315	0.0012	-0.0067
M55	-0.1929	0.0064	-0.0074	0.0076
M66	0.3568	-0.0241	0.0005	-0.0039
M77	0.1441	-0.0211	0.0097	0.0101
M88	0.2756	-0.0283	-0.0100	0.0050
MS1	1.0400	1.0368	1.0363	1.0405
M12	-0.8287	-0.8312	-0.8317	-0.8349
M23	-0.3131	-0.4741	-0.4712	-0.4630
M34	-0.5734	-0.5649	-0.5615	-0.5616
M45	-0.5474	-0.5479	-0.5467	-0.5500
M56	-0.4493	-0.4582	-0.4582	-0.4595
M67	-1.0048	-0.8143	-0.8352	-0.8293
M78	-0.8696	-0.7769	-0.7780	-0.7885
M8L	1.0960	1.0288	1.0358	1.0460
M14	-0.1780	-0.2267	-0.2239	-0.2193
M58	0.4437	0.3774	0.3714	0.3669

Chapter 6

CONCLUSIONS AND DISCUSSIONS

A novel systematic approach to analytically extracting the coupling matrix and the unloaded Q of a practical narrow band coupled resonator filter is presented. The filter diagnosis and extraction is a very important step in computer aided tuning of a microwave band pass filter. The concept of phase loading is materialized for the first time in the subject. To convert the measured data of a physical model to a circuit model, the theoretic formulas for conveniently removing the phase loading effect and the embedded transmission line from a given filter response of a physical model are developed. An analytical formula for calculating the loss factor in the system poles is also developed in the proposed approach. Being able to accurately determine the complex poles of a filter and consequently the unloaded Q values for each resonator, the analytical approach can be effectively used for the diagnosis of a lossy filter.

The proposed approach is practical to the industry and simple to use. There is no need to use non-linear optimization and no requirement for a legitimate initial value for extracting a filter response. This analytical tool will find good applications in the computer aided tuning of microwave filters.

Some of the practical issues in the implementation are listed below.

(1) Non-unique coupling structures

When the rotation sequence for a golden template is given, there is no multiple solutions. Otherwise, an optimization is required with the extracted coupling matrix as initial values.

(2) Parasite couplings

The parasite couplings can not be removed by analytic extraction. They are usually small comparing to other couplings, thus can be neglected. As a filter response approached to the ideal one, the parasite couplings are getting smaller.

Use analytic extracted coupling matrix as initial values in optimization where the parasite couplings can be forced to zero.

(3) Measurement noise

In measurement, measurement noise can be found at the region where S_{21} is lower than -60dB. Usually, this region is far away from the pass band. For interpolation and extraction, the data used are not far away from the pass band so the noise can be ignored. Also since the noise appears in S_{21} but not S_{11} or S_{22}, it can not have influences in the removing of phase loading since we use phase of S_{11} and S_{22} in this procedure.

For the measured data in pass band, which may include small noise, rational interpolation is applied before further processing and noise is reduced.

APPENDIX A: TIME DOMAIN TUNING

The analytic approach to extracting coupling matrix presented by this thesis is suitable for the tuning of narrow band filters whose poles are analytically visible in the frequency range set by vector network analyzer. This requires (1) poles are within the range of several bandwidth away from the filter's center frequency (2) the magnitude of a pole can not be lower than the noise level. In practice, when filters are first assemblies, every of its tuning screws is detuned. So an additional technique is necessary to bring all the resonant frequencies within a range. Time domain tuning introduced by J. Dunsmore [3,22] is chosen for that purpose.

Using inverse Fourier transform, time domain response can be derived from S parameters. Fig. A2 shows the time domain response of a 6th degree Chebyshev filter transformed from S11 shown in Fig. A1. The dips in the figure in t>0 are corresponding to coupled resonators from input port to output port.

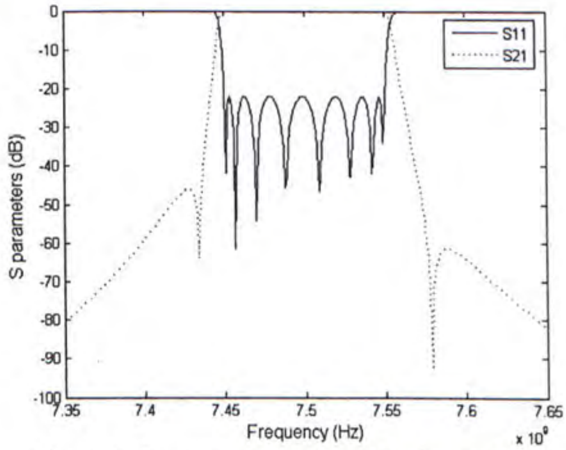

Fig. A1: S parameters of an 8th degree filter.

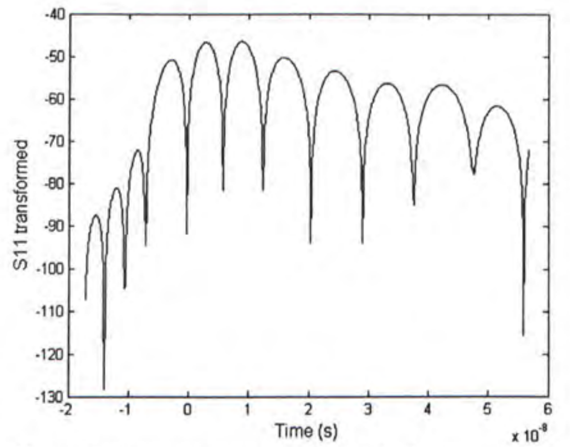

Fig. A2: Time domain response of an 8th degree Chebyshev filter

In the time domain response, start time and stop time should be chosen so that every resonator can be seen. The start time is usually a little less than zero. The stop time can be determined by filter's order using experience equations as:

$$
\begin{aligned}
&4 \le N \le 5 \qquad k = 0.9 \\
&6 \le N \le 8 \qquad k = 1.05 \\
&9 \le N \le 13 \qquad k = 1.2 \\
&T_{start} = -\frac{2N+1}{\pi^2 BW} \\
&T_{stop} = -k\frac{2N+1}{\pi^2 BW}
\end{aligned}
\tag{A.1}
$$

For filter tuning the time domain response of a golden template is used to guide the tuning process. Fig.A3 and Fig.A4 shows the comparison of the responses of the template with the one when one of the resonators (M22 in coupling matrix) is detuned. It can be conclude from the figure that the detuning of a resonator can be indicated by the changing of the corresponding dip.

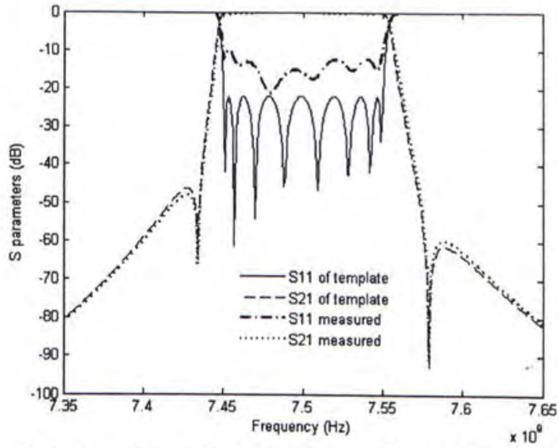

Fig. A3: S parameters of an 8th degree filter with M22 detuned.

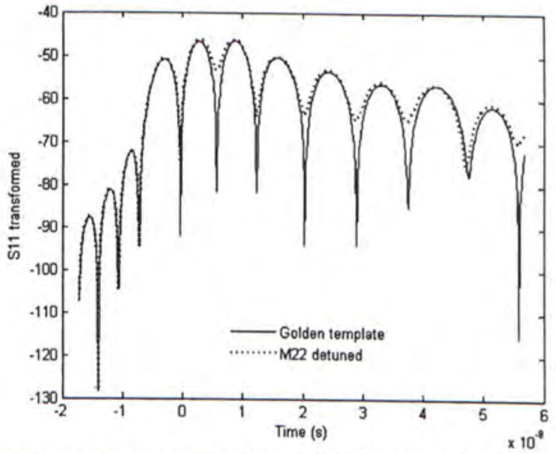

Fig. A4: Time domain response of the 8th degree filter with M22 detuned.

Fig. A5 and Fig. A6 shows the effect of changing the mainline coupling. In the figure M23 coupling is changed and it can be shown by the changing of the peak between the second and third dip.

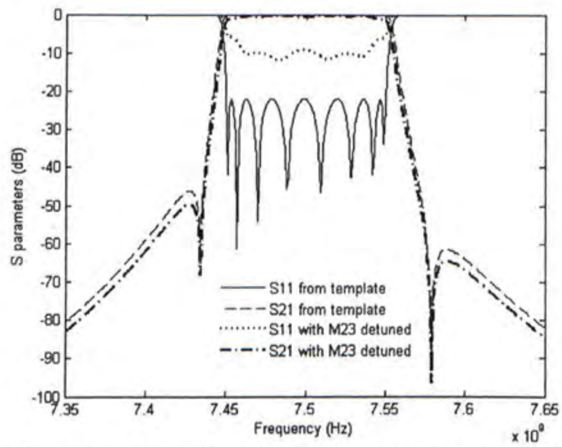

Fig. A.5: S parameters of an 8th degree filter with M23 detuned.

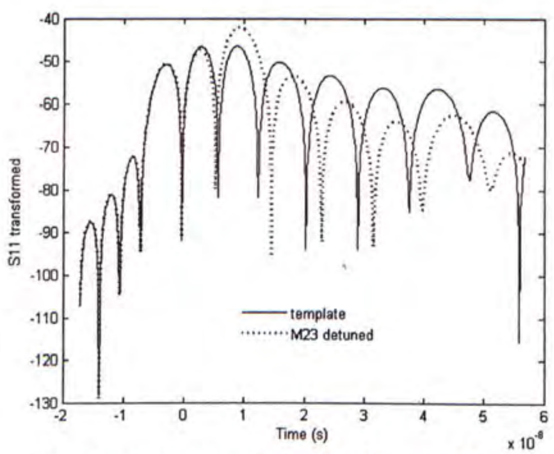

Fig. A.6: Time domain response of the 8th degree filter with M23 detuned.

Tuning process using this 8th degree filter as an example:

1. Using S11 to tune the first four resonators and S22 to tune the last four resonators.
2. The sequence of tuning is Ms1, M11, M12, M22,...
3. The purpose of time domain tuning is to bring the resonant frequencies in nearer to the pass band, so it is not necessary to tune the response exactly the same as template.

APPENDIX B: ACME USER'S MANUAL

B.1 ACME BASICS

1.1. Description of the program

Analytic Coupling Matrix Extraction (ACME) is a program that is used for the computer aided tuning of microwave band pass filters by coupling matrix extraction.

The traditional tuning approach is mainly based on the fuzzy logic that a technologist built up over years and is tedious and labor intensive. One of the difficulties is that the manual tuning is not a deterministic. ACME presents systematic analysis of the measured or simulated response of a filter.

Coupling matrix (CM) is an important reference because each of its terms corresponds uniquely to a physical element; also it has a direct and simple mathematic relation to the response. The basic idea of parameter extraction is to determine the coupling matrix from the S parameters response and compare it with the golden template. The differences between the extracted one and the golden template indicate which structure should be modified. The main approach of CAT used in the industry is based on the coupling matrix extraction using nonlinear optimization.

What can ACME do?

Basically, ACME can extract the coupling matrix from measure S parameters response and compare it with the golden template. When the response of extracted coupling matrix is fitted to the measurement with enough accuracy, the physical filter is modeled by the coupling matrix. Then ACME will show you the element (self-coupling or cross couplings) with the maximum difference, the corresponding structure in the physical filter should be tuned.

Both analytic and optimization extractions can be applied using build-in engines. The removing of phase loading and de-embedding can automatically correct the response to be fitted by a rational modal. The unloaded Q of each resonator is also determined.

The other utilities of ACME include:

- Display the response of golden template.

- Load and display S parameters from Vector Network Analyzer (Angilent E5071B, HP8510C, Angilent N5230A or Angilent E8363B) or simulation tools (Emosaic, HFSS).
- Make corrections on the response of a filter by Stoer-Bulirsch interpolation, de-embedding, and removing phase loading so that a rational modal could be built.
- Perform analytic methods or non linear optimization of coupling matrix and unloaded Q extraction.
- Simulate a coupling matrix to get its response.
- Compare the response of golden template, measurement and simulation in different concept (the coupling matrix, the magnitude and phase of S parameters, the Y parameters and the group delay).
- Perform time domain analysis on measured data.

Technologies used in ACME

- Rationalization of measured response by Stoer-Bulirsch interpolation, de-embedding and removing phase loading
- Analytic extraction of coupling matrix and unloaded Q based on pole identifications. Loss is introduced to the coupling matrix synthesis procedure by adding a real part to the poles.
- Non-linear optimization for coupling matrix extraction and de-embedding.
- Time domain analysis.

Limitations

- All the poles of Y parameters should not be too far away from pass band, that is, the filter is pretuned.
- When there is pole degeneration due to the loss, it might be required for the users to manually input some key parameter in analytic extraction.
- When loss level of the measured data is large, users might need to set the parameters for interpolation.
- When the filter is nearly tuned, that is , when the difference between extracted coupling matrix and golden template is less than 0.01, or when the return loss level of the measured data is lower than -17dB, due to the accuracy limitation, users are required to simulate the tuning using simu and find out the key element that should be tuned in the next step instead of tuning the element with maximum difference.

System requirement

The program is written and debugged in a Windows XP system.

1.2. Requirement on calibration

The coupling matrix extraction procedure is very sensitive to the phase of the input S parameters, so please pay extra attention to calibration. There is no such formula to determine if a calibration is good or not. We provide two indicators which might be used as reference.

Observe the plots of Y parameters. The real part of Y11 should be positive.

Observe the plot for power conservation. The maximum level in pass band should not vary too much. For a good calibration, the level within the passband is less than 0.02 (variations may exist due to loss).

B.2 INSTALLATIONS

A complete package contains following parts:

Programs Names	Functions
CM_extraction.exe	The user interface of ACME
for_show.exe	Display the golden template and measurement
ana.exe	Analytical extraction
opti.exe	Non-linear optimization
TD.exe	Time domain response
simu.exe	Simulation
Pic (folder)	Pictures used for the main program
Example(folder)	Input files for example

These files should be put into proper positions on your Windows system.

For system bin

- Put the for_show.exe, ana.exe, opti.exe, simu.exe and TD.exe in your bin folder such as C:\bin.
- Then add path to this folder so that these programs could be used any where in your system. Choose Windows setting panel - system - environment variable.
- Add new path to your bin folder containing the four exe files.

For CM_extraction.exe

Put CM_extraction.exe and folder pic where you want to save the measurement data. When the CM_extraction.exe is started, a folder named temp will be automatically created to store all the temporary files.

These are the descriptions for the temporary files:

file type	descriptions
.sp	File containing S parameters starting with two columns (2 and number of frequency points)
.ipt	Input file for the other .exe
.dat	File containing the group delay, Y parameters or time domain response.
.ops	Input file for Emosaic_opt.exe

B.3 GETTING STARTED

3.1. A general description

This part shows the general descriptions for the interface.

A general view of the interface

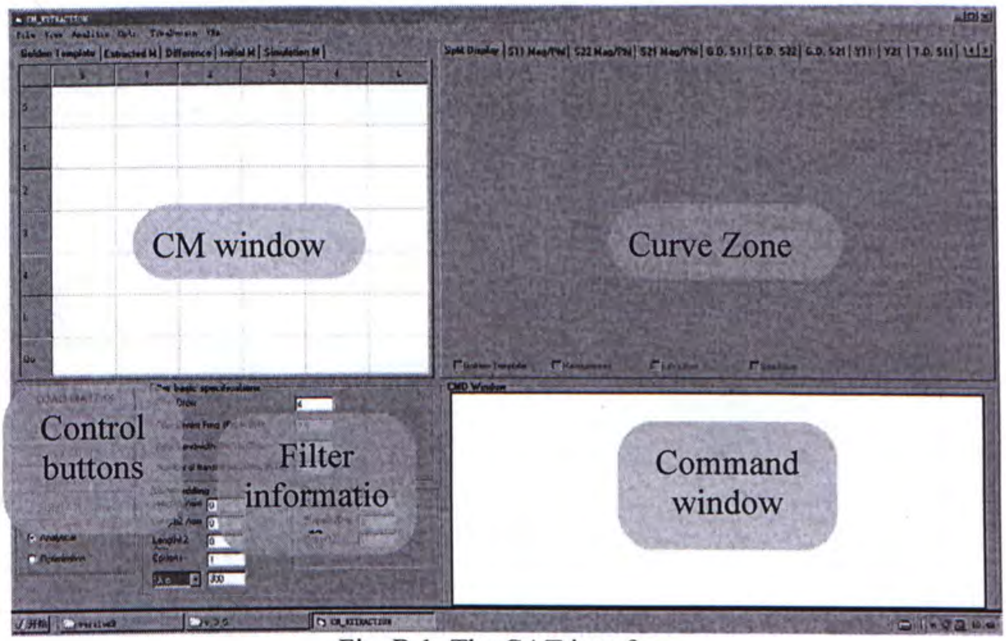

Fig. B.1: The CAT interface

Coupling matrix window

This part shows the Coupling Matrix in N+2 formation. For an Nth degree filer, there are (N+2)*(N+2) elements. The last row is the unloaded Q of the corresponding resonator. Golden template contains the designed goal and is imported from .gtp file. For a lossy design, there should be equal values of Qu as the last row.
Extracted M shows the coupling matrix from extraction (both analytic and optimization). The extraction may contain element not existing in golden template and those ones are shown in grey while the others are black.
Diff.M shows the difference between golden template and extracted M (extracted-golden). The color indicating the magnitude of the difference.
Initial shows the initial values for optimization. Its values are loaded automatically from each extraction. To make the element a variable for optimization, double click the cells in the matrix. Then input the initial value, the upper bound and lower bound in the popup window. The blue ones are the variables.
Simu.M contains the coupling matrix be used in simulation.

Curve zone

There are four sets of S parameters, the ones from golden template, from measurement, from extraction, and from simulation. These sets are shown in different colors in curve zone.

The ticks below allow choosing the sets to be displayed.

The tabs allows to choose the formats including the magnitude, phase and group delay of S11, S22, S21; the real and imaginary part of Y11 and Y21 and the time domain response.

Command window

Command windows show the information of executing the internal program.

When a text line in command starts with "!!!" , there is an error occurred. Please read the error description and change corresponding settings.

Control buttons

Load Matrix. The *.gtp file containing golden template need to be specified.
Load S para. The *.sp file containing S parameters need to be specified. If user need to load S parameters from Vector Network Analyzer, please refer settings for VNA.
Meas. Display shows the golden template and measured data to curve zone.
Extraction starts coupling matrix extraction procedure according to the method selected below (analytic or optimization).

This step will automatically give the extracted coupling matrix in folded form. If other configuration of coupling matrix is preferred, please refer to analytic setting.

The de-embedding and removing of phase loading will be performed according to build-in procedures if the values are all 0. For special cases, user may need to change those variables manually.

Simulation can plot the S parameters for a given coupling matrix to simulate the process of tuning.

Filter information

In filter basic information, the order, number of transmission zeros, the center frequency and bandwidth are loaded from .gtp file. These values may be changed.
Define de-embedding information. When there is wave-guide or coaxial cable connecting the input and output port, information about de-embedding should be given, including the length, the permittivity and cut off wavelength. If they are not given, the program will perform build-in procedures.

To optimize the length of wave-guide at ports:

Input the proper cutoff wavelength and relative permittivity for your case.
Double click the length cell
Input the initial value, the upper bound and lower bound

Define phase loading information. If they are not given, the program will perform build-in procedures.

Menu bar

Contains more specific settings which are discussed in part IV.

3.2. Instructions on settings

Analytic settings

Click Setting in analytic menu. The following form will appear.

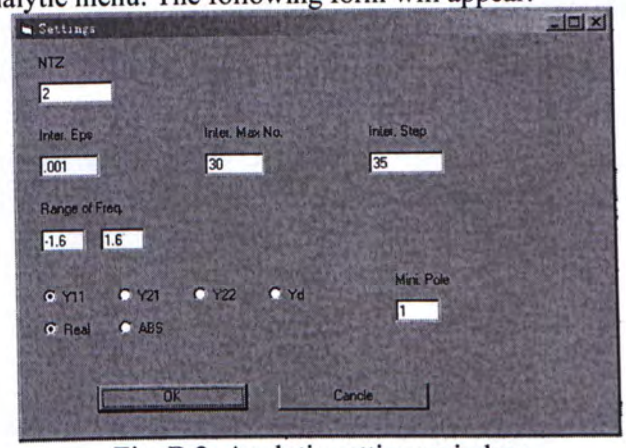

Fig. B.2: Analytic settings window

General Information	NTZ	Number of trans.zeros
Interpolation	Inter. Eps	Maximum allowed error
	Inter. Max No.	Maximum num. iteration
	Inter. Step	Number of sample
	Range of Freq.	Range of freq. in lowpass band
Pole Identification	Ys	The Y parameter used
	Re/Im	The real or imaginary part
	Min. Pole	Lowest heigh of pole

Define interpolation parameters. When data is read from VNA or sp file, rational interpolation is performed to increase the accuracy of extraction. Also when there is loss, the poles of Y parameter may degenerate. Under this condition polynomial interpolation is applied to find the hidden poles. For data from circuit modal and measurement, different parameters are needed for interpolation. So these values may need modifications according to the case working on.

Define pole identification parameters. The magnitude of poles may change according to different filters. The poles can be seen in Y parameters in curve zone.
Load rotation sequence

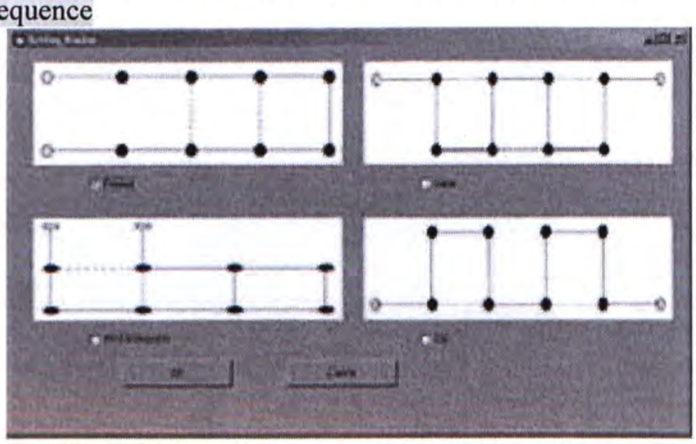

Fig. B.3: Coupling matrix configurations window

There are different configurations for filter with different order. When user need to change the folded structure into some other desired ones,

Optimization settings

Click Setting in opti. menu.

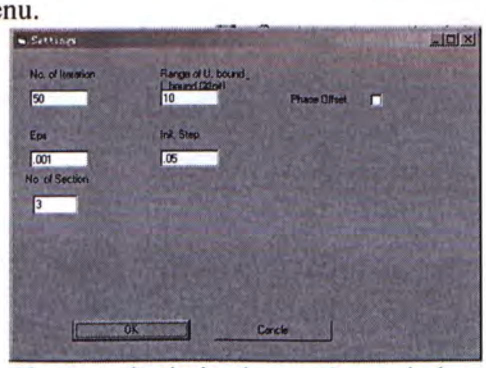

Fig. B.4: Optimization settings window

Emosaic Opt	Num. of Iteration	As the name indicate
	Range of bound	Range of variable settings for initial M
	Phase Offset	Add 180 phase offset to S21
	Eps	Maximum allowed error
	Init. Step	Initial steps
Section	Num. of sections	As the name indicate

Clicking Section in menu.

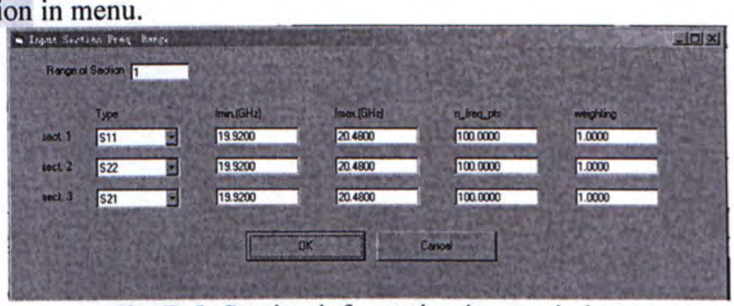

Fig. B.5: Section information input window

The number of sections is defined in Settings for optimization.

Range of Sections	Range of low and upper bound away from center frequency in the number of bandwidth
Type	Type of S parameters
fmin/fmax	Minimum/Maximum frequency for this section
n_freq_pts	Num. of equally spaced frequency points
weighting	As name indicated.

Time Domain settings

Fig. B.6: Time domain setting window

The type of S parameters used for time domain calculation can be chosen, S11, S22 or both. Sample_FFT is the number of sample used in FFT. The larger the value, the smother the curve while the time of calculation may be increased also.

VNA settings

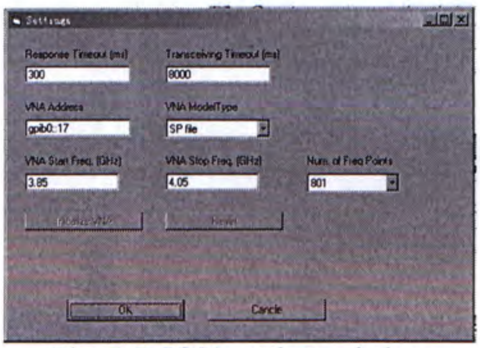

Fig. B.7: VNA settings window

Time for VNA	Response Timeout	Time delay for response
	Transceiving Timeout	Time delay for tranceiving
VNA type	VNA Address	Specified for different model
	VAN model type	As name indicated
VNA initialization	Start Freq.	Start frequency
	Stop Freq.	Stop frequency
	Num. of Freq. Pts	Num. of frequency points
	Initialize VNA	As name indicated

Choose VNA Modal Type. It require user to choose the measuring equipment. For EM simulation, we choose EMOSAIC.
Initialize VNA. This command starts VNA. If the VNA Modal is EMOSAIC, the command requires user to specify the .sp file containing the measured S parameters.

B.4 A HELLO WORLD EXAMPLE

4.1 preparations of the input files

1 .gtp file

This file contains the golden template in N+2 formation. For a complete description of golden template, the filter order, number of transmission zeros, center frequency and bandwidth should also be included.

The header contains four rows which are:

Filter order   Number of transmission zeros   Center frequency   Bandwidth

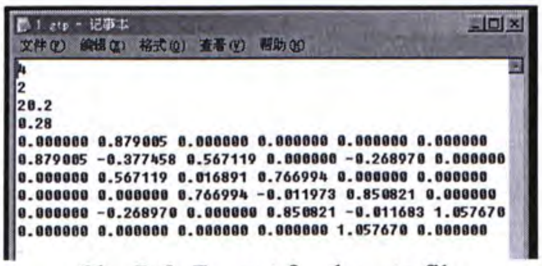

Fig. B.8: Fromat for the .gtp file

2 .sp file
.sp file contains the measured S parameters. The format is:

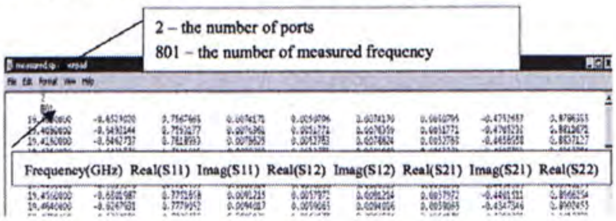

Fig. B.9: Format for the .sp file

2 .fst file
This file contains all the settings for an example and is saved and loaded by users. When the settings for one example is adjusted properly, users may use Save all to save all the information of this example including golden template, de-embedding, phase loading, and all settings. These information could be re-loaded by Load all.

4.2. Procedures of coupling matrix extraction

We used a 4th filter as our first example. The .gtp file and the .sp file can be found in folder example.

Click load Matrix
Click load S para.
Click Meas. Display
Click Extraction

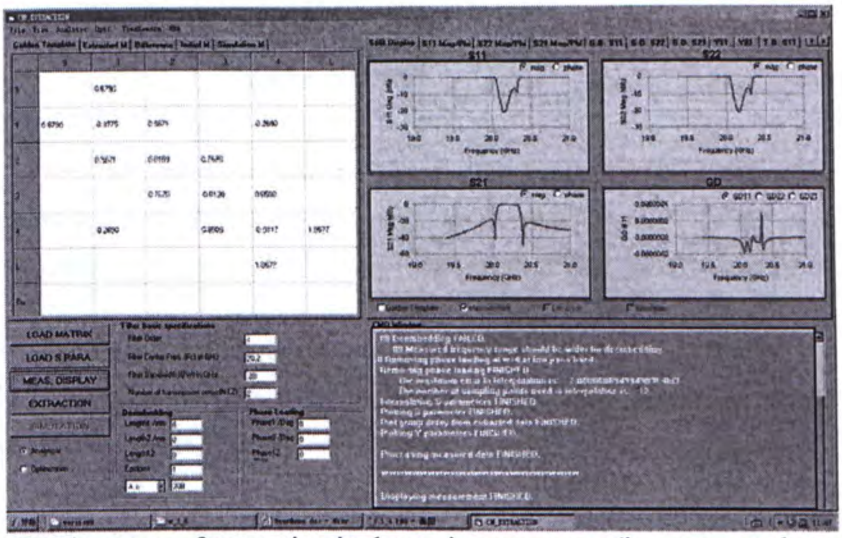

Fig. B.10: The curve of extraction is shown in curve zone (in green overlapped with measurement)

BIBLIOGRAPHY

1. J. B. Ness, "A unified approach to the design, measurement, and tuning of coupled-resonator filters," *IEEE Trans. Microwave Theory Tech.* MTT-46, pp. 343-351,1998

2. G. Pepe, F.-J. Görtz, H. Chaloupka, "Sequential tuning of microwave filters using adaptive models and parameter extraction," *IEEE Trans. Microwave Theory Tech.* MTT-53, pp. 22-31,2005

3. J. Dunsmore, "Simplify filter tuning in the time domain," *Microwaves RF*, vol. 38, no. 4, pp. 68-84, 1999

4. R. J. Cameron, C. M. Kudsia, R. R. Mansour, *Microwave filters for communication systems*, Wiley, 2007, ch. 8.

5. M. Yu, and M. Ismail, "Automated tuning and optimization of microwave filters and multiplexers," 2003 IEEE International Microwave Symposium, workshop, June 2005.

6. M. Kahrizi, S. S.-Naeini, S. K. Chaudhuri and R. Sabry, "Computer diagnosis and tuning of RF and microwave filters using model-based parameter estimation," *IEEE Trans. on Circuit and systems-I,* vol.49, no.9, pp. 1263-1270,2002

7. A. G. Lampérez, T. K. Sarkar and M. S. Palma, "Generation of accurate rational models of lossy systems using the Cauchy method," *IEEE Microwave and wireless components letters,* vol. 14, no. 10, 2004

8. P. Harscher, R. Vahldieck and S. Amari, "Automated filter tuning using generalized low-pass prototype networks and gradient-based parameter extraction," *IEEE Trans. Microwave Theory Tech.* MTT-49, pp. 2532-2538,2001

9. H.-T. Hsu, H.-W. Yao, K. A. Zaki and Ali E. Atia, "Computer-Aided diagnosis and tuning of cascaded coupled resonators filters," *IEEE Trans. Microwave Theory Tech.* MTT-50, pp. 1137-1145, 2002

10. H.-T. Hsu, Z. Zhang, K. A. Zaki and Ali E. Atia, "Parameter extraction for symmetric coupled-resonator filters", *IEEE Trans. Microwave Theory Tech.*, MTT-50, pp. 2971-2978, 2002

11. W. Meng and K.-L. Wu, "Analytical diagnosis and tuning of narrowband multicoated resonator filters," *IEEE Trans. Microwave Theory & Tech.*, vol. 54, no. 10, pp. 3765-3771, Oct. 2006.

12. F. Seyfert, L. Baratchart, et.al, "Extraction of coupling parameters for microwave filters: determination of a stable rational model from scattering data," *IEEE MTT-S Digest*, TU1B-5, pp. 25-28, 2003

13. R. J. Cameron, C. M. Kudsia, R. R. Mansour, *Microwave filters for communication systems*, Wiley, 2007, ch. 3.

14. D. M. Pozar, *Microwave Engineering*, John Wiley, 2004, ch.4.

15. A.E. Atia, A. E. Williams and R.W. Newcomb, "Narrow-band multiple-coupled cavity synthesis", *IEEE Trans. On Circuit and System*, vol. cas-21, no. 5, pp. 649-655, Sep 1974.

16. A. E. Williams, W. G. Bush and R.R. Bonetti, "Predistortion technique for multicoupled resonator filters methods for Chebyshev filtering function", *IEEE Trans. Microwave Theory Tech.*, MTT-33, pp. 402-407, May 1985.

17. J. Stoer, R. Bulirsch, *Introduction to Numerical Analysis*, third edition, Springer 2002. ch. 2.

18. G. A. Baker and P. Graves-Morris, *Padé approximats*, Cambridge U. P. 1996.

19. B. Gustavsen and A. Semlyen, "Rational approximation of frequency domain responses by vector fitting," *IEEE Transactions on Power Delivery*, vol. 14, no. 3, pp. 1052-105, July 1999.

20. Y. Ding, K.-L. Wu, D. G. Fang, "A broad-band adaptive-frequency-sampling approach for microwave-circuit EM simulation exploiting Stoer-Bulirsch algorithm," *IEEE Trans. Microwave Theory Tech.* MTT-51, pp. 928-934, 2003

21. R.J. Cameron, M. Yu, "Design of manifold coupled multiplexers, IEEE Microwave Magazine," *IEEE Microwave Magazine,* pp. 46-57, Oct 2007.

22 J. Dunsmore, "Tuning band pass filters in the time domain," *IEEE MTT-S Int. Microwave Symp. Digest*, pp. 1351-1354,1999